Sulfoquinovose is differently degraded by the mouse and human gut microbiota and not metabolized by the host

Julia Krasenbrink[1,2], Buck T. Hanson[1,3], Anna S. Weiss[4§], Sabrina Borusak[5,6], Tomohisa Sebastian Tanabe[1], Michaela Lang[1], Georg Aichinger[7,8] , Bela Hausmann[9,10], David Berry[1,9], Andreas Richter[11], Doris Marko[7], Marc Mussmann[1], David Schleheck[5,6], Bärbel Stecher[4,12,13], Alexander Loy[1,9]*

[1] University of Vienna, Centre for Microbiology and Environmental Systems Science, Division of Microbial Ecology, Vienna, Austria
[2] University of Vienna, Doctoral School in Microbiology and Environmental Science, Vienna, Austria
[3] Bioscience Division, Los Alamos National Laboratory, Los Alamos, New Mexico, USA
[4] Max von Pettenkofer Institute of Hygiene and Medical Microbiology, Faculty of Medicine, Ludwig Maximilian University, Munich, Germany
[5] Department of Biology, University of Konstanz, Konstanz, Germany
[6] Konstanz Research School Chemical Biology, University of Konstanz, Konstanz, Germany
[7] Department of Food Chemistry and Toxicology, University of Vienna, Austria
[8] Department of Health Sciences and Technology, ETH Zurich, Switzerland
[9] Joint Microbiome Facility of the Medical University of Vienna and the University of Vienna, Vienna, Austria
[10] Division of Clinical Microbiology, Department of Laboratory Medicine, Medical University of Vienna, Vienna, Austria
[11] University of Vienna, Centre for Microbiology and Environmental Systems Science, Division of Terrestrial Ecosystem Research, Vienna, Austria
[12] German Center for Infection Research (DZIF), Partner Site Munich, Munich, Germany
[13] Chair of Intestinal Microbiome, School of Life Sciences, Technical University of Munich, Germany

*Corresponding author: Alexander Loy alexander.loy@univie.ac.at

[§]Current affiliation:
Anna S. Weiss, Microbial Systems Ecology Group, Institute of Biogeochemistry and Pollutant Dynamics, Department of Environmental Systems Sciences, ETH Zurich, Zurich, Switzerland

Abstract

Sulfoquinovose (SQ) is a green-diet-derived sulfonated glucose and a selective substrate for few human gut bacteria. Complete anaerobic SQ degradation via interspecies metabolite transfer to sulfonate-respiring bacteria produces hydrogen sulfide, which has dose- and context-dependent health effects. Here, we studied potential SQ degradation by the mammalian host and the impact of SQ supplementation on human and murine gut microbiota diversity and metabolism. $^{13}CO_2$ breath tests with germ-free C57BL/6 mice gavaged with ^{13}C-SQ were negative. Also, SQ was not degraded by human intestinal cells *in vitro*, indicating that SQ is not directly metabolized by mice and humans. Addition of increasing SQ concentrations to human fecal microcosms revealed dose-dependent responses of the microbiota and corroborated the relevance of *Agathobacter rectalis* and *Bilophila wadsworthia* in cooperative degradation of SQ to hydrogen sulfide via interspecies transfer of 2,3-dihydroxy-1-propanesulfonate (DHPS). Similar to the human gut microbiome, the genetic capacity for SQ or DHPS degradation is sparsely distributed among bacterial species in the mouse gut. *Escherichia coli* and *Enterocloster clostridioformis* were identified as primary SQ degraders in the mouse gut. SQ and DHPS supplementation experiments with conventional laboratory mice and their intestinal contents showed that SQ was incompletely catabolized to DHPS. Although some *E. clostridioformis* genomes encode an extended sulfoglycolytic pathway for both SQ and DHPS fermentation, SQ was only degraded to DHPS by a mouse-derived *E. clostridioformis* strain. Our findings suggest that SQ is solely a nutrient for the gut microbiota and not for mice and humans, emphasizing its potential as a prebiotic. SQ degradation by the mouse microbiota differs from the human gut microbiota by absence of DHPS degradation activity. Hence, the microbiota of conventional laboratory mice does not fully represent the

SQ metabolism in humans, indicating the need for alternative model systems to assess the impact of SQ on human health. This study advances our understanding of how individual dietary compounds shape the microbial community structure and metabolism in the gut and thereby potentially influence host health.

Key words

Sulfoquinovose, prebiotic, hydrogen sulfide, organosulfonate, sulfur metabolism, gut microbiome

Introduction

The sulfonated glucose sulfoquinovose (SQ) is an abundant sulfur molecule in the global sulfur cycle. As the polar headgroup of the sulfonolipid sulfoquinovosyldiacylglycerol (SQDG), an estimated 10 billion tons of SQ is synthesized annually by photosynthetic organisms such as plants, algae, and cyanobacteria [1]. SQDG is located in thylakoid membranes and maintains the activity and structural integrity of photosystem II [2–5]. Sulfoglycolytic microorganisms can cleave SQ from SQDG or other SQ glycosides via a sulfoquinovosidase. Two types of sulfoquinovosidase enzymes are known. The YihQ sulfoquinovosidase belongs to glycoside hydrolase family 31 [6] and the NAD^+-dependent SqgA sulfoquinovosidase belongs to glycoside hydrolase family 188 [7]. To date, six microbial SQ degradation pathways have been described. In two pathways, SQ is catabolized aerobically to sulfite by individual organisms using an alkanesulfonate monooxygenase [8] or an iron- and alpha-ketoglutarate-dependent alkanesulfonate dioxygenase [9]. The other pathways require syntrophic interspecies metabolite transfer of C_2- or C_3-organosulfonates for complete degradation. The sulfo-

84 Embden-Meyerhof-Parnas pathway generates the C_3-organosulfonates 2,3-
85 dihydroxypropane-1-sulfonate (DHPS) or 3-sulfolactate (SL) during aerobic or anaerobic
86 growth [10,11]. The sulfo-Entner-Doudoroff-pathway degrades SQ aerobically to SL [12]. The
87 sulfofructose-transaldolase pathway produces SL aerobically and SL or DHPS anaerobically
88 [13,14]. The sulfo-transketolase pathway degrades SQ to two molecules of the C_2-
89 organosulfonates isethionate or, putatively, sulfoacetate [11]. In these pathways, the residual
90 carbon skeleton (either C_3 or C_2) enters the central carbon metabolism while
91 organosulfonates are excreted.
92
93 DHPS is a key metabolite of SQ-degrading human gut bacteria [15]. Four pathways for
94 anaerobic DHPS degradation are currently known. Two of these pathways are utilized by
95 select sulfite-reducing bacteria (*Desulfovibrio*, *Bilophila*) and result in the intracellular
96 formation of sulfite, which is subsequently respired to hydrogen sulfide (H_2S). In *Desulfovibrio*
97 strain DF1, DHPS is degraded to pyruvate and sulfite via 3-sulfolactaldehyde and SL [16]. In
98 *Bilophila wadsworthia*, DHPS is cleaved to hydroxyacetone and sulfite [15,17]. Some
99 fermenting bacteria, such as *Klebsiella oxytoca* and *Hungatella hathewayi*, can degrade DHPS
100 by reducing it to 3-hydroxypropane-1-sulfonate (3-HPS) via sulfopropionaldehyde in a third
101 pathway [17]. In a fourth, bifurcated pathway in *Enterococcus gilvus*, DHPS is converted to
102 both 3-HPS and 3-sulfopropionate [18]. In the human gut, *B. wadsworthia* may use 3-
103 sulfopropionate, but not 3-HPS, as a terminal electron acceptor resulting again in H_2S
104 formation [18]. The strictly anaerobic mouse gut bacterium *Taurinivorans muris* encodes
105 another potential DHPS degradation pathway, but did not degrade DHPS in growth tests [19].
106 However, this pathway was thus far only proven in aerobic bacteria, which have the

107 sulfopropanediol-3-dehydrogenase HpsN to oxidize (*R*)-DHPS to (*R*)-sulfolactate [20], which is
108 then cleaved to pyruvate and sulfite by sulfolactate-sulfolyase SuyAB [21].
109
110 As a component of edible green plants and algae, SQDG is part of the human and animal diet.
111 While the capability of mammalian cells to metabolize SQ remains unclear, SQ is a selective
112 substrate for a few but abundant human gut bacteria [15]. *Agathobacter rectalis* (formerly
113 *Eubacterium rectale*) and *B. wadsworthia* were identified as main primary and secondary SQ
114 degraders in human fecal microcosms, respectively. Nearly half of the high-quality *A. rectalis*
115 genomes from a human microbiome database [22] encoded SQ degradation via the
116 sulfofructose-transaldolase pathway, though this potential was rare among other human gut
117 bacteria, with only 0.5% of species-level genome bins containing the pathway. Despite its
118 limited genomic prevalence, the sulfofructose-transaldolase pathway ranked among the top
119 third most abundant microbial pathways in fecal metatranscriptome datasets of four human
120 cohorts. This highlights SQ degradation as a core function of the human gut microbiome, with
121 *A. rectalis* and *Faecalibacterium prausnitzii* contributing most to its transcription [15]. Primary
122 SQ degraders are generally associated with beneficial host effects [23,24] and thus SQ is a
123 candidate prebiotic. However, excessive stimulation of secondary, H_2S-producing SQ
124 degraders may be harmful as H_2S has dose-dependent impacts on host health [25]. At low
125 nano- to micromolar concentrations, H_2S has predominantly beneficial effects [26]. H_2S serves
126 as an energy source for mitochondria, as a cellular antioxidant, and as a gasotransmitter in
127 mammals [27]. Additionally, H_2S may prevent colonization by pathogens by inhibiting their
128 aerobic respiration [28]. At high micro- to millimolar concentrations produced by the gut
129 microbiota [26], however, H_2S may disrupt disulfide bonds in the intestinal mucosal layer,
130 thus enabling bacterial penetration [29], and can lead to cell death by inhibiting cytochrome

131 *c* [30]. Overabundance of H_2S-producing bacteria, such as *B. wadsworthia*, is considered as a
132 potential driver of gut inflammation [29,31,32].
133
134 Here, we assessed the prebiotic potential of SQ by studying its degradation and metabolism
135 in humans and mice using both human and mouse gut content microcosm experiments, as
136 well as *in vivo* interventions in conventional and germ-free mice. We elucidated the role of
137 mammalian cells in SQ metabolism through *in vitro* cultures and stable isotope-tracing in
138 germ-free mice. We show that SQ is not degraded by the host, establish a minimum SQ
139 concentration that impacts the human gut microbiota, and uncover fundamental differences
140 in the bacterial SQ metabolism between wild type mice and humans.
141

142 Materials and Methods

143 Human cell culture

144 HT-29, a human colorectal adenocarcinoma cell line (German Collection of Microorganisms
145 and Cell Cultures, Germany), was cultured in Dulbecco's Modified Eagles Medium (DMEM),
146 which contains 25 mM glucose, supplemented with 10% (v/v) fetal calf serum and 1% (v/v)
147 penicillin/streptomycin at 37°C and 5% CO_2 under humidified conditions. All components
148 were purchased from Invitrogen™ Life Technologies (Germany). Cells were regularly
149 monitored for mycoplasma contamination.
150 To investigate whether human intestinal cells degrade SQ, HT-29 cells were grown in DMEM
151 or in glucose-free DMEM either supplemented with 25 mM glucose, 25 mM SQ, or left
152 unamended. Supernatants were sampled after 0, 1, 6, 24, and 48 h and stored at -20°C for
153 metabolite analysis by capillary electrophoresis.

154 To study the potential inhibitory effect of SQ on the growth of HT-29 cells, 7,500 cells were
155 seeded per well and incubated in DMEM medium supplemented with glucose or SQ at three
156 concentrations (2.5 mM, 25 mM, 250 mM). In three independent experiments, duplicate
157 incubations (n = 6) were performed for all treatments. Protein production was measured as a
158 proxy for growth after 3, 5, and 7 days of incubation using sulforhodamine B colorimetric
159 assays as described previously [33]. Briefly, plates were washed with 1x PBS twice and cells
160 were fixed with a 5% trichloroacetic acid solution. Plates were dried overnight at room
161 temperature. Then, the plates were stained with 0.4% (w/v) sulforhodamine B for 1 h. After
162 washing twice with water and twice with 1% (v/v) acetic acid, the stain was eluted using a 10
163 mM Tris buffer (pH 10). Absorbance was measured at 570 nm and normalized to the solvent
164 control (1% v/v DMSO) to assess the impact of treatments on cell growth.
165

166 **Germ-free mouse experiment and $^{13}CO_2$ breath test**

167 Six germ-free male C57BL/6 mice (6–20 weeks old), were housed under sterile conditions in
168 flexible film isolators (North Kent Plastic Cages, England) or in Han-gnotocages (ZOONLAB
169 GmbH, Germany). Mice were kept on a twelve-hour light-dark cycle at 20.5-23.5°C and 45-
170 65% humidity, with autoclaved water and Mouse-Breeding complete feed (Ssniff, Germany)
171 provided *ad libitum*. Mice were scored twice daily for their health status, and sterility was
172 checked monthly during housing, before the experiment, and during the experiment using
173 qPCR with universal bacterial 16S rRNA gene primers [34,35]. Mice were randomly assigned
174 to two treatment groups and kept in separate cages. The administered substrates were either
175 10 mg of fully ^{13}C-labeled D-glucose (Sigma-Aldrich, Germany) or 10 mg of fully ^{13}C-labeled
176 SQ, which was synthesized from fully ^{13}C-labeled D-glucose following an established protocol

177 [36]. Each treatment group received their substrate dissolved in 100 µl sterile water
178 (Ampuwa; Fresenius Kabi, Germany) via gavage. Respired air from individual mice was
179 sampled for CO_2 stable isotope analysis prior to gavage (baseline) and at 1, 3, 6, 9, 12, and 24
180 h post-gavage. For breath air sampling, individual mice were placed in an airtight one-liter
181 container sealed with a lid fitted with a rubber stopper for approximately 2 minutes. Separate
182 containers were used for each treatment group to avoid cross-contamination between
183 groups. Gas samples (15 ml) were taken at 30 and 90 seconds and injected entirely into pre-
184 vacuumed exetainers (12 ml) creating an overpressure to prevent leakage from ambient air
185 into the exetainers. Ambient air samples were taken before the experiment for blank
186 measurements. If feasible, fecal samples were collected to validate sterility of mice and for
187 metabolite analysis. $^{13}CO_2$ concentrations were measured in the gas samples using isotope
188 ratio mass spectrometry (GasBench II headspace sampler connected to a Delta V Advantage
189 isotope mass spectrometer; Thermo Fisher Scientific, Germany). $^{13}CO_2$ production rates per
190 minute were calculated from the differences in $^{13}CO_2$ (atom percent excess) between the two
191 samples taken at 30 s and 90 s.
192

193 **Anoxic *in vitro* gut microcosm incubations and pure culture growth tests**

194 All anoxic incubations and growth tests were performed in an anaerobic tent (Coy Laboratory
195 Products, United States) operated with a gas mix of 85% N_2, 10% CO_2 and 5% H_2. The H_2 levels
196 in the tent atmosphere ranged between 1.5 and 2.5%.
197 Fecal samples were collected from five human individuals, who had not taken antibiotics in
198 the three months before sampling. Samples were stored at 4°C for maximally 24 h before
199 processing. All samples were pooled, and 3.9 g of fecal mass was homogenized in oxygen-free

200 30 mM bicarbonate buffer (pH 6.8). This fecal slurry (1.32 mg/ml) was distributed into 20 ml
201 Hungate tubes (final volume: 15 ml) and sealed with butyl-rubber stoppers and screw-on
202 caps. Triplicate microcosms were amended with 10 mM, 1 mM, 0.1 mM, or 0.01 mM SQ
203 (MCAT GmbH, Germany). One microcosm was left unamended (negative control). Tubes were
204 incubated at 37°C and subsamples (1 ml) were collected after 0, 3, 6, 9, 12, 16, and 24 h. From
205 each subsample, 20 µl was used for sulfide quantification. The remaining subsample was
206 centrifuged at 11,000 x g for 5 min at 4°C. Biomass-free supernatants were stored at -20°C for
207 subsequent capillary electrophoresis. Cell pellets were frozen at -80°C for DNA extraction.
208
209 In two independent experiments, we sampled intestinal contents of conventional C57BL/6
210 wild type mice to create mouse gut content slurries. Mice were housed under specific-
211 pathogen-free conditions with standard chow diet (Ssniff V1534, Ssniff, Germany) and water
212 *ad libitum*, in compliance with Federation of European Laboratory Animal Science
213 Associations guidelines. After euthanasia, mice were dissected in an anaerobic chamber.
214 In the first experiment, ten mice (4 females, 6 males, 8–10 weeks old) were dissected, and
215 their small intestinal, cecal and large intestinal contents were pooled and homogenized with
216 oxygen-free 1x PBS (pH 7.4). The gut content slurry (5.25 mg/ml) was distributed into 20 ml
217 Hungate tubes (final volume: 10 ml). Mouse gut microcosms were left unamended or
218 amended with 10 mM SQ or 10 mM DHPS. All treatments were performed in triplicate.
219 Hungate tubes were sealed with butyl-rubber stoppers and screw-on caps and incubated at
220 37°C. Subsamples were collected at 0, 24, 48, and 96 h, and sulfide was quantified in 20 µl of
221 subsample.
222 In the second experiment, eight mice (4 females, 4 males, 8–10 weeks old) were dissected,
223 and their small intestinal (2.2 g) and cecal contents (5.9 g) were separately pooled. Small

224 intestine and cecal contents were homogenized with oxygen-free 1x PBS (pH 7.4) and
225 transferred into 20 ml Hungate tubes (final volume: 15 ml) with a concentration of 4.9 mg/ml
226 and 5.15 mg/ml of small intestinal and cecal content, respectively. Both sets of microcosms
227 were left unamended or amended with 10 mM SQ, and sealed with butyl-rubber stoppers
228 and screw-on lids for incubation at 37°C. All treatments were performed in triplicate.
229 Subsamples (1 ml) were taken at 0, 24, 120, and 220 h. In both experiments, subsamples were
230 centrifuged at 11,000 x g for 5 min at 4°C. Pellets were stored for DNA extraction at -80°C and
231 biomass-free supernatants were stored at -20°C for metabolite analyses.
232
233 *Enterocloster clostridioformis* YL32 (DSM 26114) and *Faecalibaculum rodentium* ALO17 (DSM
234 103405) were each grown in triplicate cultures in 100% and 30% brain heart infusion broth
235 with or without 10 mM SQ at 37°C in gas-tight Hungate tubes. Anoxic and autoclaved
236 ultrapure water was used for dilution of the medium. Growth was monitored by measuring
237 optical density at 600 nm. Identities of grown strains were confirmed by direct Sanger
238 sequencing (Microsynth GmbH, Austria) of 16S rRNA gene amplicons.
239

240 **Conventional wild type mouse experiment**

241 Fifteen conventional C57BL/6 wild type mice (6-8 weeks) were maintained with *ad libitum*
242 water and autoclaved mouse chow (Ssniff V1534, Ssniff, Germany). The day/night cycle was
243 14/10 hours, and environmental conditions were maintained at 20–24°C with 45–65%
244 humidity. After one week of acclimatization, mice were randomly assigned to three groups
245 (two males and three females each) with no significant differences in weight between groups.
246 Two treatment groups were gavaged with 1 mg or 10 mg SQ in 100 µl aqueous solutions,

247 while the third, control group was gavaged with 100 µl autoclaved tap water. Fecal samples
248 were collected 0, 3, 6, 9, 12, and 24 h post-gavage. General discomfort of treated mice was
249 assessed by observing them after gavage and throughout the experiment for signs of reduced
250 mobility, scruffy fur, hunched posture or changes in facial expression. Mice were sacrificed
251 and dissected after 24 h. Fecal samples and intestinal contents were immediately stored at -
252 80°C for metabolite analysis and 16S rRNA gene amplicon sequencing.
253

254 **Metabolite analysis**

255 For sulfide quantification, 20 µl subsamples were added to 300 µl 2 g/l zinc acetate solution
256 in the anaerobic tent. Fixed samples were quantified colorimetrically using the Infinite M
257 Nano+ microplate reader (Tecan, Austria), as described previously [37].
258 Capillary electrophoresis was used to quantify metabolites in the supernatants of human cell
259 cultures, in gut microcosms, in bacterial pure cultures, and in the fecal samples of germ-free
260 and conventional mice. Concentrations of SQ, SL, DHPS, lactate, and the short-chain fatty
261 acids (SCFAs) formate, succinate, acetate, propionate, butyrate, and valerate were quantified
262 using a 7100 capillary electrophoresis system (Agilent, United States). Mouse fecal samples
263 were prepared by adding 40 µl of ultrapure water to 0.01 g of feces. After mixing, samples
264 were centrifuged at 11,000 x g for 10 min at 4°C and supernatants were stored at -20°C. For
265 analysis, culture supernatants or metabolite extracts from fecal samples were diluted 1:5-
266 1:20 in ultrapure water containing 0.1 mM of an internal standard. Caproate, valerate or
267 succinate was used as an internal standard and was selected based on the sample
268 background. Analyte standard mixtures were prepared in concentrations of 0.025 mM, 0.05
269 mM, 0.1 mM, 0.25 mM, 0.5 mM and 1 mM. An organic acid buffer (Agilent, United States)

270 was used as a running buffer. The instrument's bare fused silica capillary (75 µm inner
271 diameter, 72 cm effective length; Agilent, United States) was flushed within the system for
272 four minutes as part of the preconditioning process before each measurement. Samples were
273 then injected at 50 mbar for five seconds. Measurements were performed at –25 kV, 100 µA,
274 and 6 W.
275 SQ and its degradation products DHPS, SL, isethionate, 3-HPS, 3-sulfopropionate, and
276 sulfoacetate in mouse gut content microcosms, *E. clostridioformis* pure cultures, and in fecal
277 samples of germfree and conventional mice were additionally quantified using liquid
278 chromatography-mass spectrometry. Samples were prepared by centrifuging at 18,000 x g for
279 5 minutes at 4°C. The supernatants were then diluted 1:10 with ultrapure water and mixed at
280 a 7:3 (v/v) ratio with ≥ 99.9% acetonitrile containing 6.7 mM para-toluenesulfonate as internal
281 standard. Samples were quantified using a LCMS-2020 single quadrupole mass spectrometer
282 system (Shimadzu, Japan) consisting of LC-40B XR pumps, a SIL-40C XR autosampler, a CTO-
283 40S column oven (heated to 30°C) and a MS-2020 electrospray ionization mass spectrometer.
284 Organosulfonate separation was carried out on an iHILIC-Fusion(+) column (100 × 2.1 mm, 3.5
285 µm, 100 Å), as described previously [38].
286

287 **16S rRNA gene amplicon sequencing and real-time PCR**

288 DNA extraction and 16S rRNA gene amplicon sequencing was performed by the Joint
289 Microbiome Facility of the Medical University of Vienna and the University of Vienna under
290 the project numbers JMF-2012-06 (human fecal microcosms), JMF-2108-01 (conventional
291 mouse experiment), JMF-2212-09 (mouse gut content microcosms). DNA was extracted with
292 the QIAamp Fast DNA Stool Mini Kit according to the manufacturer's protocol (Qiagen GmbH,

293 Austria). Extraction contamination was controlled for using blank extractions containing kit-
294 provided buffers alone. An established two-step PCR-barcoding method (H_515F_mod-5'-
295 (head) GCT ATG CGC GAG CTG C - GTG YCA GCM GCC GCG GTA A and H_806R_mod-5'-(head)
296 TAG CGC ACA CCT GGT A - GGA CTA CNV GGG TWT CTA AT) was used for 16S rRNA gene
297 amplicon sequencing of bacteria and archaea [39]. Prior to preparing the sequencing libraries,
298 barcoded amplicon libraries were normalized with the SequalPrep normalization plate kit and
299 subsequently pooled (TrueSeq Nano Kit; Illumina, United States) [39,40]. Amplicon
300 sequencing was performed on the MiSeq (V3, 600 cycles; Illumina, United States) and results
301 were analyzed according to the procedures outlined previously [39]. Amplicon sequence
302 variants (ASVs) were inferred using the DADA2 workflow [41] and taxonomically classified
303 with the SILVA database (release 138). Sequencing libraries were rarified and analyzed with
304 the software packages phyloseq (v1.42.0) [42] and vegan (v2.6-4) [43] for RStudio
305 (rstudio.com, R version 4.2.2). Principal coordinate analysis was performed using a Bray-Curtis
306 dissimilarity matrix computed with phyloseq. DESeq2 (v1.38.3) was used to perform
307 differential abundance analyses between treatment groups and time points [44].
308 In the human fecal microcosm experiment, ASV abundance at each time point and treatment
309 was compared to two controls: Its corresponding baseline at 0 h, and to the abundance in the
310 0.01 mM SQ incubation at the same time point. Notably, the 0.01 mM SQ incubation was used
311 as control because (i) metabolite data showed no significant differences compared to the
312 unamended control and (ii) only one control incubation was sequenced. The baseline at 0 h
313 served as control to identify ASVs with an increased abundance compared to the beginning
314 of the experiment. ASVs significantly enriched in both analyses were considered responsive
315 to the amendment. For the mouse gut content microcosm experiments, each treatment was
316 evaluated against the unamended control at each time point. In the conventional mouse

317 experiment, ASV abundance was compared to the baseline at 0 h for each treatment.
318 However, ASVs were considered significantly responsive to the amendment only, if they were
319 not also significantly enriched in the unamended control over time. Adjusted *p*-values of <0.01
320 were considered significant. The taxonomic classification of enriched ASVs in all experiments
321 was verified by Blastn against the NCBI 16S rRNA sequences database, excluding uncultured
322 and environmental sample sequences [45].
323
324 The total 16S rRNA gene copies were quantified by real-time PCR (CFX96 Real-Time System;
325 Bio-Rad Laboratories Ges.m.b.H, Austria). PCR reactions consisted of 10 µl iQ SyBr Green Mix
326 2x, 0.8 µl of each primer (0.4 µM), 6.4 µl sterile nuclease-free water, and 2 µl DNA extract.
327 The universal primers 515F (5'-GTG YCA GCM GCC GCG GTA A-3') [46] and 806R (5'-GGA CTA
328 CNV GGG TWT CTA AT-3') [47] targeting bacteria and archaea were used. The PCR program
329 started with an initial denaturation step at 95°C for 5 min followed by 40 cycles of 95°C for
330 30 s, 55°C for 30 s, and 72°C for 30 s. Final elongation was performed at 72°C for 2 min. A
331 negative control, i.e. water as template, was included in each run. Genomic DNA
332 of *Escherichia coli* K12 was used to prepare a standard serial dilution series of 10^9 (15.4 ng/µl
333 DNA of the standard) to 10^3 copy numbers of the 16S rRNA gene to generate a standard curve,
334 which was linear across the entire dilution series. The 16S rRNA gene copy numbers of
335 selected ASVs were calculated by multiplying their relative abundances with the total 16S
336 rRNA gene abundances determined by real-time PCR.
337

338 **Analysis of genomes from the mouse microbiome**

339 High-quality mouse microbiota-derived bacterial genomes were downloaded from the Mouse
340 Gastrointestinal Bacteria Catalogue (n=26640) [48]. Open reading frames were determined
341 using prodigal and subsequently annotated via HMSS2 [49]. Additional hidden Markov models
342 were generated for SQDG and DHPS conversion related proteins not represented in HMSS2,
343 as described previously [50]. Among others, this included isethionate reductase IsrBHDK [51],
344 DHPS-sulfolyase HpsGH, DHPS-dehydratase HpfGH [17], sulfopropionaldehyde reductase
345 HpfD, succinate semialdehyde dehydrogenase Ssadh [52], DHPS dehydrogenase DhpA, 3-
346 sulfolactaldehyde dehydrogenase SlaB [16] and sulfoquinovosidase SqgA [7] (Table S1). For
347 all hidden Markov models, a general bitscore cutoff of 100 was chosen to detect homologs.
348 All hits were tested for co-location in the respective genome with a maximum distance of
349 3500 nucleotides between genes, as described before [50]. The resulting gene clusters were
350 then searched for patterns of genes with the same sequential occurrence using a custom
351 implementation of the colinear syntenic blocks finder algorithm [53], with a tolerance of two
352 gene insertions and a length of four co-located genes. This was done to ensure enzyme
353 function in the respective metabolism by sequence similarity and genetic vicinity.

354

355 **Results**

356 **SQ is not degraded by human HT-29 cells *in vitro***

357 To test whether SQ is degraded by human intestinal cells, we incubated HT-29 human
358 colorectal cancer cells with and without SQ. SQ concentrations in cell culture supernatants
359 from both SQ-supplemented DMEM and glucose-free DMEM remained unchanged

360 throughout the experiment (Figure 1 a, b). Lactate was only produced in glucose-containing
361 incubations (Figure 1 c, d). The effect of increasing glucose or SQ concentrations on HT-29 cell
362 growth in DMEM was similar for both substrates. Protein production was fully inhibited only
363 in cultures treated with very high, non-physiological concentrations (250 mM) of glucose or
364 SQ (Figure 1 e, f). Overall, these findings suggest that SQ is not degraded and metabolized by
365 human cells *in vitro*.
366

367 **^{13}C-labeled SQ is not respired to ^{13}C-CO_2 by germ-free mice**

368 Next, we employed stable isotope tracing with ^{13}C-SQ in germ-free mice to study potential SQ
369 degradation by mammalian cells *in vivo*. Germ-free mice received a single dose (10 mg) of
370 either fully labeled ^{13}C-SQ or ^{13}C-glucose and their respired air and fecal samples were
371 subsequently collected over a 24-hour period for $^{13}CO_2$ breath tests and metabolite analysis,
372 respectively. Mice administered ^{13}C-SQ did not produce $^{13}CO_2$. Contrarily, mice receiving ^{13}C-
373 glucose produced up to 117 µg $^{13}CO_2$/min at one hour post-gavage (Figure 1 g). In mice
374 gavaged with ^{13}C-SQ, SQ was detected in fecal samples already one hour after its
375 administration (Figure 1 h). Yet, SQ degradation metabolites were not detected in the feces.
376

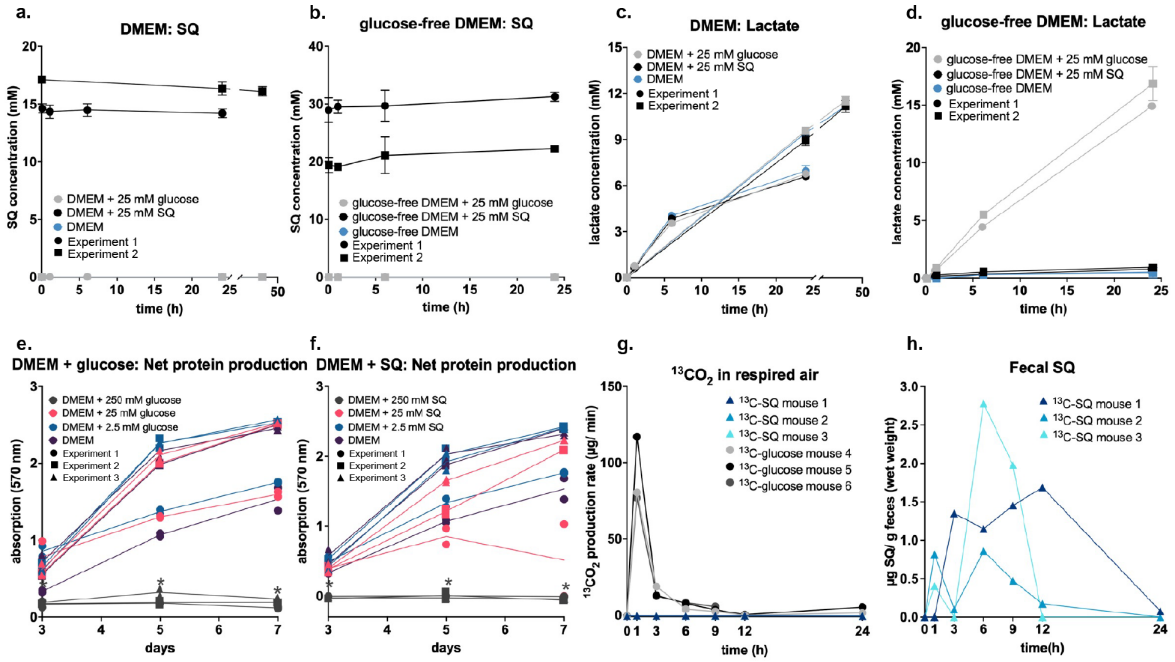

Figure 1: SQ was not metabolized by human intestinal cells and germ-free mice. SQ was not degraded by HT-29 cells in DMEM medium amended with 25 mM SQ (shown in black) (a). SQ was not degraded by HT-29 cells in glucose-free DMEM medium amended with 25 mM SQ (shown in black) (b). HT-29 cells produced lactate independent of the treatment in DMEM medium (c). In glucose-free DMEM, HT-29 cells produced lactate only in incubations amended with 25 mM glucose (shown in grey) (d). Protein production was inhibited in incubations with 250 mM glucose (shown in dark grey), but not in incubations with 25 mM glucose (shown in pink) and 2.5 mM glucose (shown in blue) (e). Protein production was inhibited in incubations with 250 mM SQ (shown in dark grey), but not in incubations with 25 mM SQ (shown in pink) and 2.5 mM SQ (shown in blue) (f). Each germ-free mouse (n = 3 per group) was gavaged with 10 mg of fully labeled ^{13}C-glucose or ^{13}C-SQ. (g). Glucose, but not SQ, was respired by germ-free mice as shown by $^{13}CO_2$ production via breath air isotope analysis. SQ was repeatedly detected in the feces of all mice gavaged with ^{13}C-SQ within 24 h after the gavage (h). In a., b., c., and d., lines show averages of triplicate incubations with error bars representing one standard deviation. Two experiments were conducted varying only slightly in the sampling time points. Different data point shapes indicate the two experiments. In e. and f., lines show averages of duplicate measurements and data points show individual values. Different data point shapes represent the three conducted experiments. Asterisks mark significant differences between a treatment group and the control (DMEM medium without amendment) at each time point. Significant differences were determined by ANOVA with Dunnett's post hoc test. Adjusted *p*-values smaller than 0.05 were regarded as significant. SQ, sulfoquinovose; DMEM, Dulbecco's Modified Eagle Medium.

Response of the microbiota to different doses of SQ in human fecal microcosms

We performed anoxic incubations with human fecal microcosms to assess the dose-dependent effects of SQ (0.01 mM, 0.1 mM, 1 mM, and 10 mM) on metabolite production and gut microbiota composition (Figure 2 a). Only the microcosms with high SQ concentrations (1 mM, 10 mM) consistently showed significant differences in metabolite levels compared to the unamended control (Figure S1). The temporal dynamics of SQ

403 degradation and the production of metabolic products were consistent between the 1 mM
404 and 10 mM SQ treatments (Figure 2 b, c). SQ was mostly degraded within 12 h, coinciding
405 with the production of DHPS. In comparison, SL and sulfide were produced later and
406 represented only a smaller fraction of the produced sulfur metabolites within the 24 h
407 incubation. SQ, DHPS, and SL were not detected in the unamended control incubation (Figure
408 2 d). The production of acetate and butyrate, known SQ degradation products [15,16,38],
409 increased significantly in the 1 mM and 10 mM SQ treatments compared to the unamended
410 control (Figure 2 e, f).
411 Changes in total microbial abundance during the 24 h incubation period were quantified by
412 16S rRNA gene-targeted real-time PCR (Figure 2 g). Gene copy numbers decreased in
413 microcosms without SQ and with 0.01 or 0.1 mM SQ and remained transiently constant in
414 microcosms with 1 mM SQ. A significant increase in gene copy numbers was only observed in
415 microcosms with 10 mM SQ.
416 We performed 16S rRNA gene amplicon sequencing and differential abundance analyses to
417 identify ASVs with increased relative abundance in SQ-amended incubations and thus a
418 possible role in SQ degradation. Significantly enriched ASVs were only detected in incubations
419 with concentrations of 0.1 mM SQ or higher; one, two, and fourteen ASVs were enriched in
420 microcosms with 0.1, 1, and 10 mM SQ, respectively (Table S2, Figure S2). *Escherichia/Shigella*
421 ASV 8 was enriched at all three SQ concentrations, *Waltera intestinalis* ASV 7 was enriched at
422 1 and 10 mM SQ, while the following ASVs were only enriched at 10 mM SQ: *A. rectalis* ASV
423 1, *Alistipes shahii* ASV 2, *Ruminococcus bromii* ASV 3, *Oscillospiraceae* ASV 5, *B. wadsworthia*
424 ASV 6, *Enterocloster citroniae* ASV 9, *Phocaeicola dorei* ASV 4, *Phocaeicola massiliensis* ASV
425 12, *Phocaeicola vulgatus* ASV 14, *Bacteroides xylanisolvens* ASV 10, *Bacteroides caccae* ASV
426 11, and *Bacteroides ovatus* ASV 13. Close relatives of some of the enriched ASVs (Figure 2 h,

427 i, j) have been physiologically confirmed to degrade SQ (*A. rectalis*, *E. coli*) or DHPS (*B.*
428 *wadsworthia*) [10,15]. Furthermore, members of the genera *Enterocloster* and *Ruminococcus*
429 encode the sulfofructose-transaldolase pathway [15]. Together with a member of *Alistipes*,
430 members of these genera/species have also previously been significantly enriched in human
431 fecal microcosms amended with 10 mM SQ [15]. ASVs related to these taxa generally showed
432 a continuous increase in absolute abundance over the 24 h incubation, which coincided with
433 the kinetics of SQ disappearance and DHPS production (Figures 2 and S2). In contrast, ASVs of
434 *Phocaeicola* and *Bacteroides* showed an initial spike in absolute abundances at 6 h followed
435 by a decline, suggesting they are not directly involved in SQ degradation (Table S2, Figure S2).
436 Type strain genomes of the most closely related *Alistipes*, *Waltera*, *Bacteroides* or *Phocaeicola*
437 species do not encode known SQ or DHPS degradation pathways.

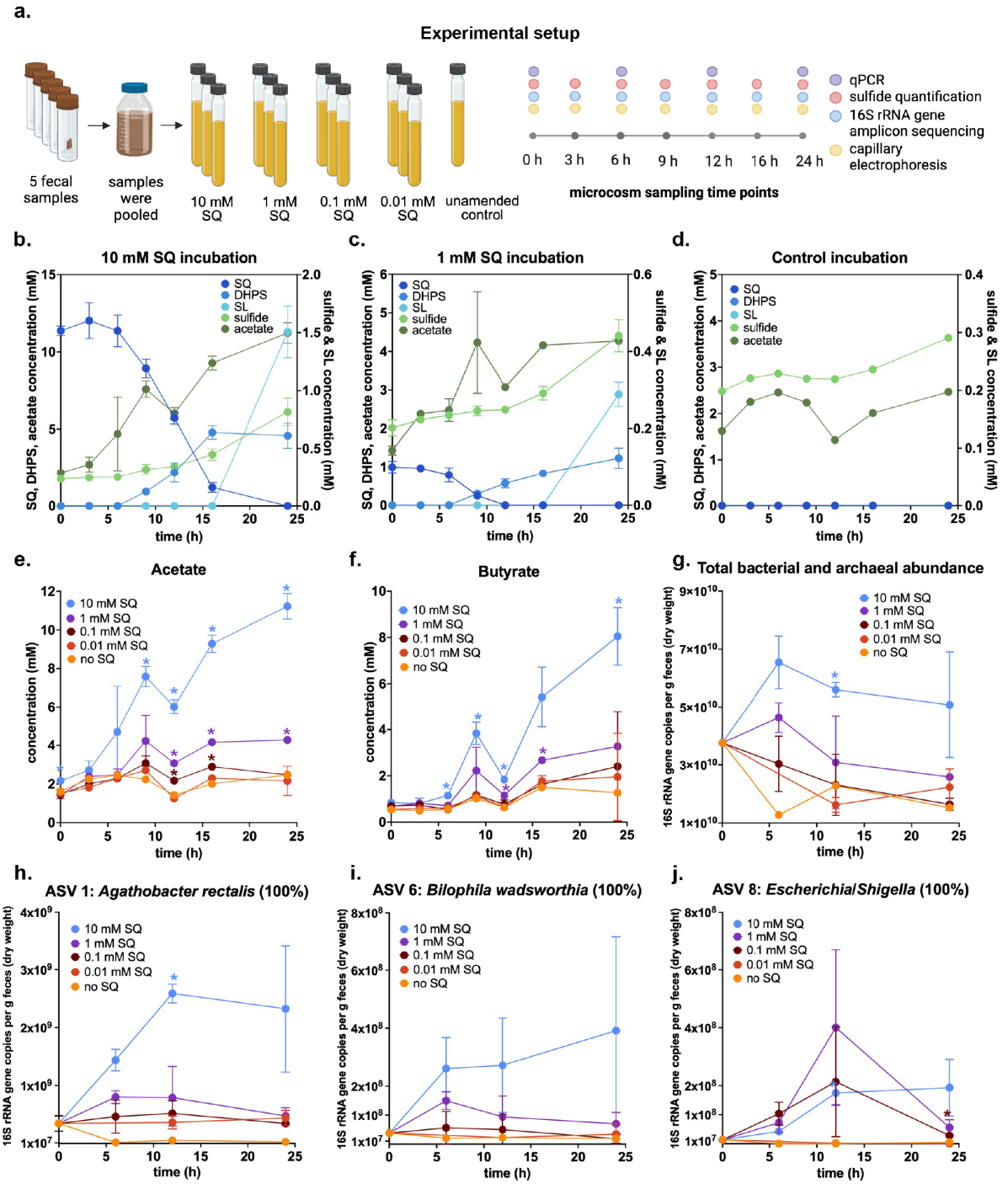

Figure 2: Metabolite dynamics and differential responses of microbiota members to different doses of SQ in 24 h human fecal microcosm incubations. Overview of the experimental and analytical approach (created with biorender.com) (a). Sulfur metabolite dynamics in incubations amended with 10 mM SQ (b), 1 mM SQ (c), and in the unamended control (d). SQ, DHPS, and SL were not detected in unamended control microcosms. Higher doses of SQ led to increased concentrations of acetate (e) and butyrate (f). No significant differences in acetate concentrations were detected between incubations with 0.01 mM SQ (shown in red) and unamended controls (shown in orange). No significant differences in butyrate concentrations were detected between incubations with 0.1 mM SQ (shown in dark red) or 0.01 mM SQ (shown in red) and unamended controls (shown in orange). Changes in absolute bacterial and archaeal 16S rRNA gene copy numbers in the microcosm incubations with different SQ doses (g). Changes in the absolute abundance of *A. rectalis* ASV 1 (h), *B. wadsworthia* ASV 6 (i), and *Escherichia/Shigella* ASV 8 (j). The 16S rRNA gene sequence similarity (%) to the closest, named relative is shown for each ASV. In b., c., e., f., g., h., i., and j., the lines show the average of triplicate incubations with error bars representing one standard deviation. Only a single incubation was performed for the unamended control microcosm. Coloured asterisks show significant differences between the respective treatment (n = 3) and the retrospectively designated control incubations (n = 4, consisting of three 0.01 mM SQ incubations and one unamended control) at individual time points. Significant differences

were determined by ANOVA with Dunnett's post hoc test. Adjusted *p*-values smaller than 0.05 were regarded as significant. SQ, sulfoquinovose; DHPS, 2,3-dihydroxypropane-1-sulfonate; SL, 3-sulfolactate; ASV, amplicon sequencing variant.

Incomplete SQ degradation in mouse gut content microcosms

Two independent microcosm experiments were performed with pooled gut contents of mice and amended with SQ or DHPS to investigate the SQ metabolism (Figure 3 a). In experiment 1, microcosms containing entire gut contents were incubated with either 10 mM SQ or 10 mM DHPS. Following a lag phase of over 24 hours, SQ degradation to DHPS was observed in SQ-amended incubations at a near 1:1 ratio, as measured by liquid chromatography-mass spectrometry (Figure 3 b). SL, sulfoacetate, and 3-HPS were not detected. Yet, small amounts of isethionate (0.01 mM after 48 h and 0.02 mM after 96 h) were detected (Figure S3). Sulfide concentrations in SQ-amended microcosms increased slightly, remaining below 1 mM, and did not correlate with SQ degradation in timing or stoichiometry. Capillary electrophoresis analysis of SCFAs showed an increase in acetate production in SQ-amended incubations, from 5 mM to 11.1 mM over 96 h, compared to the control incubation, from 2.6 mM to 4.3 mM (Figure 3 b). Concentrations of DHPS and acetate remained constant in DHPS-amended incubations (Figure 3 c). Sulfide concentrations were significantly higher in DHPS-amended incubations compared to SQ-amended incubations and unamended controls. However, the small increase from 0.2 mM to 0.5-0.6 mM sulfide in the DHPS-amended incubations compared to 0.3-0.4 mM sulfide in the unamended control did not suggest a quantitative turnover of DHPS to sulfide (Figure 3 c). SQ and DHPS were not detected in the unamended control incubations, and sulfide concentrations remained below 0.4 mM (Figure 3 d).

Microbial abundances decreased over time in all microcoms, but remained significantly higher in SQ incubations from 48 h onwards (Figure S4). Microbial abundances decreased from 1.8 ± 0.7 x 10^{10} 16S rRNA gene copies/g dry weight to 5.2 ± 1.0 x 10^{9} 16S rRNA gene copies/g dry

478 weight in SQ-amended microcoms and to 5.3 ± 1.4 x 10^8 16S rRNA gene copies/g dry weight
479 in the unamended controls.
480 Differential abundance analysis of 16S rRNA gene amplicon sequencing data identified nine
481 ASVs enriched in the 10 mM SQ incubations compared to unamended controls (Figure S5).
482 *Escherichia/Shigella* ASV 8 had the highest $\log_2$ fold change of all enriched ASVs and its
483 absolute abundance dynamic corresponded to the turnover of SQ into DHPS (Figure 3 b, e).
484 Other enriched ASVs included *Lachnospiraceae* ASV 15, *Bacteroides acidifaciens* ASV 16,
485 *Bacteroides* ASV 19, *F. rodentium* ASV 17, *Coprobacillaceae* ASV 18, *Ruminococcus* ASV 20,
486 *Prevotellaceae* ASV 21, and *P. vulgatus* ASV 14 (Table S3). Notably, *Escherichia/Shigella* ASV 8
487 and *P. vulgatus* ASV 14 were enriched in both human fecal microcosms and mouse gut
488 content microcosms with SQ. In contrast to SQ-amended incubations, temporal changes in
489 microbial community composition in the DHPS-amended incubations were indistinguishable
490 from control incubations and no ASVs were identified as enriched (Figure 3 f).
491
492 For experiment 2, separate microcosms for small intestinal contents and cecal contents were
493 each incubated with 10 mM SQ and analyzed for changes in microbial community composition
494 compared to unamended control incubations. Microbial 16S rRNA gene copy numbers
495 decreased in control incubations, while remaining rather constant in cecal incubations with
496 SQ or decreased less in small intestinal incubations with SQ compared to the control (Figure
497 S4). Seven ASVs were significantly enriched in small intestinal incubations and four ASVs in
498 cecal incubations. ASVs in small intestinal incubations were *Enterococcus* ASV 22 and 23,
499 *Enterocloster* ASV 24, 25, and 26, *Ligilactobacillus* ASV 27, and *Akkermansia muciniphila* ASV
500 28 (Figure 3 g, Table S3). In cecal incubations, enriched ASVs belonged to *Escherichia/Shigella*
501 ASV 8, *Parabacteroides distasonis* ASV 29 and 30 and, *Enterocloster* ASV 25 (Figure 3 h, i, Table

502 S3). In contrast to the other ASVs, the absolute abundances of *Ligilactobacillus* ASV 27 and *A.*

503 *muciniphila* ASV 28 decreased during the incubation and thus are unlikely to be involved in

504 primary SQ degradation (Figure S6).

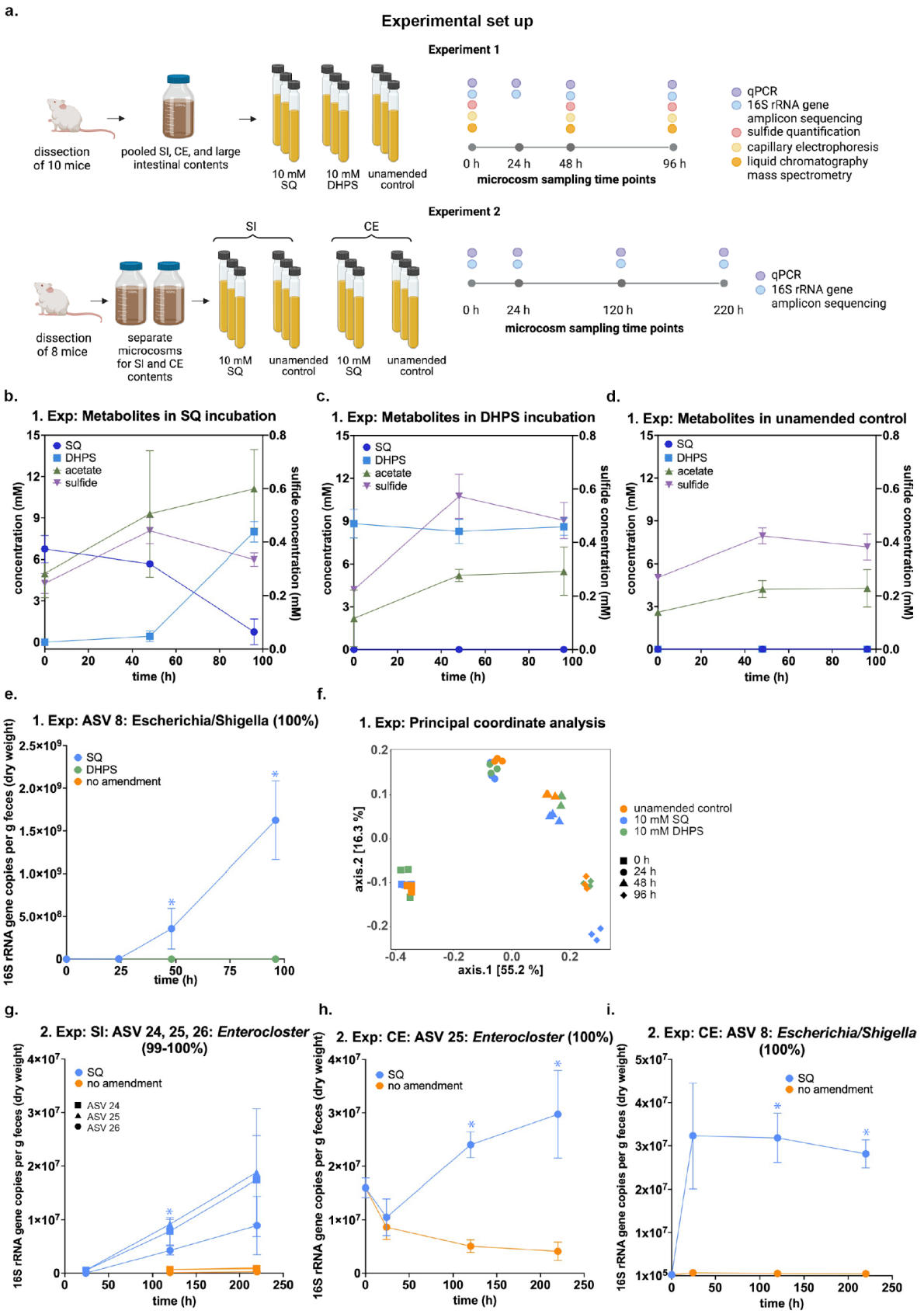

Figure 3: Metabolite dynamics and differential responses of microbiota showed that SQ, but not DHPS, was degraded in murine gut content microcosms. Overview of the experimental and analytical approach (created with biorender.com) (a). Metabolite dynamics in gut content microcosms (Experiment 1: pooled small intestinal, cecal, and large intestinal contents) incubated with 10 mM SQ (b), 10 mM DHPS (c), and without amendment (control) (d). SQ and DHPS were not detected in

510 control incubations. Calculated absolute 16S rRNA gene abundance of *Escherichia/Shigella* ASV 8 in incubations of
511 experiment 1 (e). Principal coordinate analysis plot of beta diversity (Bray-Curtis dissimilarity) of 16S rRNA gene amplicon
512 data from incubations of experiment 1 (f). Calculated absolute 16S rRNA gene abundance of selected ASVs that were
513 significantly enriched in SQ-amended mouse small intestinal content and cecum content incubations of experiment 2 (g-i).
514 The 16S rRNA gene sequence similarity (%) to the closest, named relative is shown for each ASV. The lines in b., c., d., e., g.,
515 h. and i. show averages of triplicate incubations with error bars representing one standard deviation. Coloured asterisks
516 show significant differences between the respective treatment and the unamended control at individual time points.
517 Significant differences were either determined by two-way ANOVA with Dunnett post hoc test (1. experiment: pooled gut
518 content) or by multiple unpaired t-tests with Holm-Šidák post hoc test (2. experiment: small intestine and cecum). Adjusted
519 *p*-values smaller than 0.05 were regarded as significant. SQ, sulfoquinovose; DHPS, 2,3-dihydroxypropane-1-sulfonate; Exp,
520 experiment; SI, small intestine; CE, cecum; ASV, amplicon sequencing variant.

521

522 **SQ is degraded to DHPS in conventional wild type mice**

523 To investigate SQ metabolism by the mouse gut microbiota *in vivo*, we gavaged a single dose
524 of either 1 mg SQ or 10 mg SQ to conventional wild type laboratory mice and collected fecal
525 samples up to 24 h post-gavage (Figure 4 a). Mice fed with SQ showed no signs of digestive
526 problems or general discomfort. The consistency of fecal pellets remained stable throughout
527 the experiment, with no difference between the tap water control and SQ-treated mice. Fecal
528 metabolites were analyzed via capillary electrophoresis as well as liquid chromatography-
529 mass spectrometry (Table S4). SQ was detected in mice receiving 10 mg SQ between 3 and 6
530 h post-gavage, while DHPS appeared at 6 h and remained detectable in some mice until the
531 end of the experiment (Figure 4 b, Figure S7). Additionally, taurine as well as small amounts
532 of 3-sulfolactate, sulfoacetate, and isethionate were measured via liquid chromatography-
533 mass spectrometry in mice receiving 10 mg SQ (Table S4). Taurine and isethionate were
534 detected already at the beginning of the experiment, indicating that the presence of these
535 metabolites was independent from SQ addition. Temporal dynamics of SCFA concentrations,
536 total 16S rRNA gene copy numbers, and microbial composition were not significantly different
537 between the three treatment groups (Figure 4 c - g).

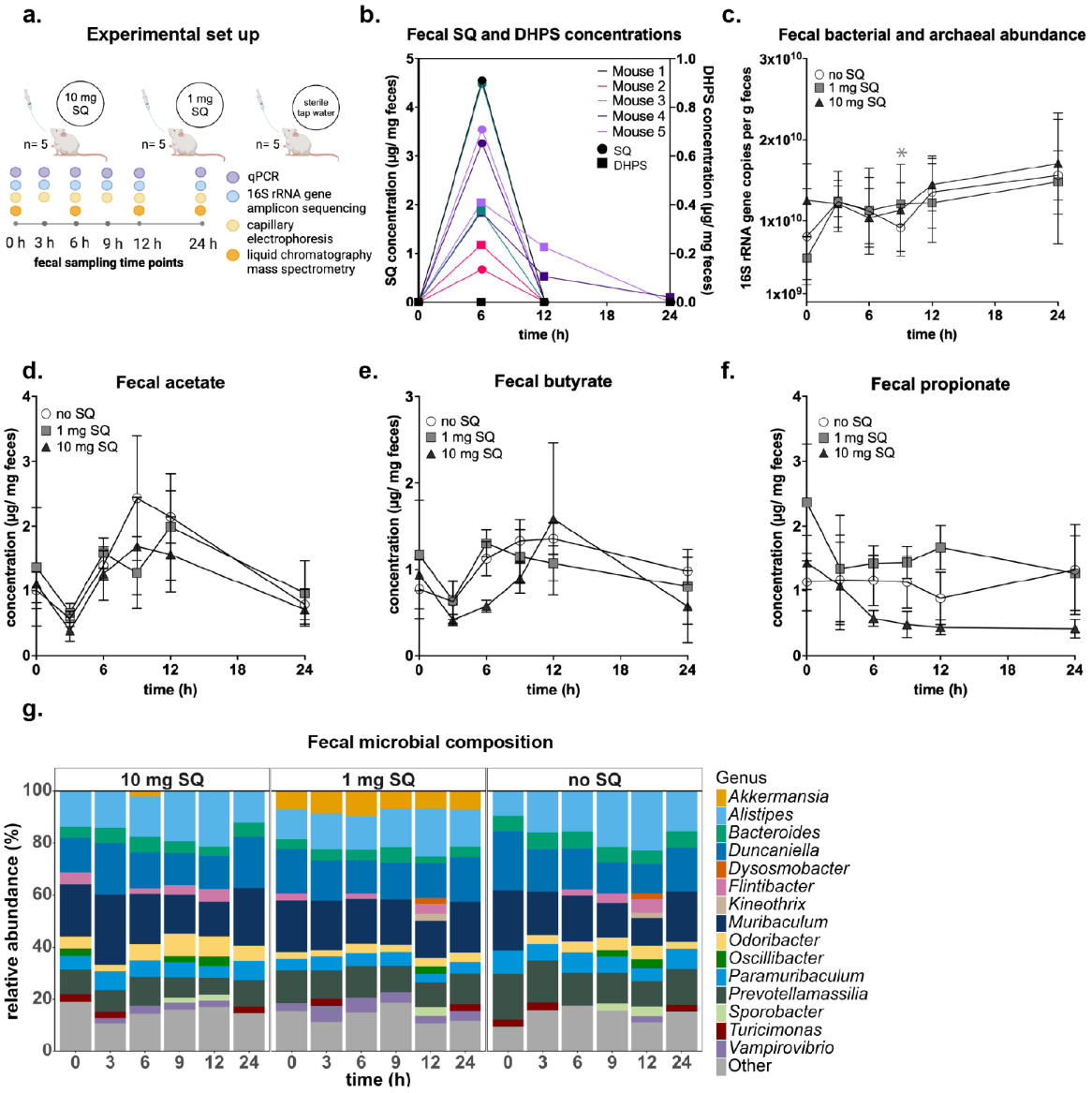

Figure 4: Fecal metabolite and microbial community dynamics of conventional wild type mice over 24 h after receiving a single dose of SQ. Overview of the experimental and analytical approach (created with biorender.com) (a). Concentrations of SQ (circles) and DHPS (boxes), as analyzed by liquid chromatography-mass spectrometry, in feces of mice (n = 5) that each received a single dose of 10 mg SQ by gavage (b). Metabolite concentrations of all treatment groups, as analyzed by capillary electrophoresis, are depicted in Supplementary Table S4 and Figure S7. Total bacterial and archaeal 16S rRNA gene copy numbers in feces of the three treatment groups (c). Five biological replicates were measured in triplicate qPCR assays. The line shows the mean and the error bars represent one standard deviation. Concentrations of acetate (d), butyrate (e), and propionate (f) in feces of the three treatment groups. Mean values of five biological replicates are shown and error bars depict one standard deviation. Mean relative 16S rRNA gene abundance of dominant bacterial genera in feces of the three treatment groups (g). All genera below an abundance of 2% are summarized in 'Other'. All data refer to the wet weight of the feces. Asterisks show significant differences between the respective treatment and the tap water control at individual time points. Significant differences in c., d., e., and f. were determined by ANOVA with Dunnett's post hoc test. Adjusted *p*-values smaller than 0.05 were regarded as significant. SQ sulfoquinovose, DHPS 2,3-dihydroxypropane-1-sulfonate.

553 **SQDG/SQ and DHPS degradation pathways are encoded in few bacterial**
554 **genomes from the mouse gut**

555 We comprehensively examined the genetic potential for SQDG/SQ and DHPS degradation in
556 the mouse microbiota by analyzing the collection of 26640 metagenome-assembled genomes
557 (MAGs) from the Mouse Gastrointestinal Bacteria Catalogue for presence of the respective
558 pathways [49]. Our analysis revealed SQDG/SQ and DHPS degradation pathways in only 0.3%
559 (n=76) and 0.2 % (n=48) of all MAGs and in 16 (1.5%) and 8 (0.7%) of the 1094 species-level
560 genome bins, respectively (Figure 5 a, b). The sulfofructose-transaldolase pathway was
561 encoded in 57 MAGs, primarily from *E. clostridioformis*, *Clostridium symbiosum*, and *E.*
562 *aldenensis*, and represented the most prevalent SQDG/SQ degradation pathway in the mouse
563 microbiome (Figure 5 a). The sulfo-Embden-Meyerhof-Parnas pathway was encoded in 13
564 *Enterobacteriaceae* MAGs. The sulfo-transketolase pathway was encoded in 6 *Oscillibacter*
565 MAGs. Key enzymes in DHPS degradation pathways (Figure 5 c) were encoded in 48 MAGs
566 across five genera. These included 16 MAGs with *hpsN*, 12 MAGs with *dhpA*, 10 MAGs with
567 *hpfGH*, 8 MAGs with *hpsGH*, and 2 MAGs with both *hpsGH* and *dhpA* (Figure 5 b). These
568 pathways could generate sulfite intracellularly and were present in the sulfidogenic genera
569 *Desulfovibrio*, *Taurinivorans*, *Mailhella*, and *Bilophila* that employ a DsrAB-dissimilatory
570 sulfite reductase to respire sulfite to H_2S [15,16,19]. Nine *E. clostridioformis* MAGs and one *E.*
571 *aldenensis* MAG encoded the fermentative *hpfGHD* pathway along with the sulfofructose-
572 transaldolase pathway, suggesting these bacteria may ferment SQ via DHPS also to 3-HPS [17].

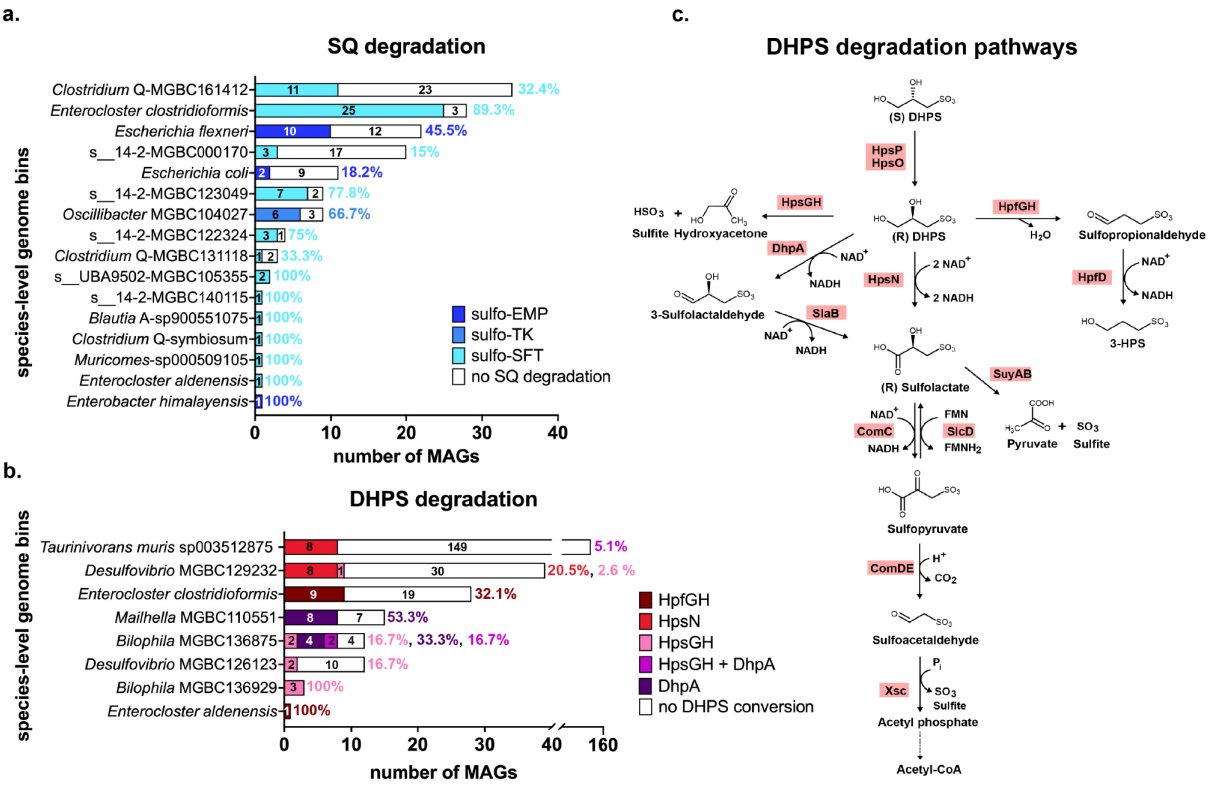

Figure 5: Analysis of microbial genomes revealed genetic SQDG/SQ and DHPS degradation potential is sparsely distributed in the mouse microbiome. Distribution of SQDG/SQ (a) and DHPS (b) degradation potential across a collection of 26,640 microbial MAGs from the mouse intestinal tract. Species-level genome bins are ordered based on the total number of genomes. The total and relative (%) number of genomes that encode a specific SQDG/SQ or DHPS pathway (shown in different colors) is indicated for each species-level genome bin. Sixteen (represented by 76 MAGs) and eight (represented by 48 MAGs) species-level genome bins, contained complete gene clusters for SQDG/SQ and DHPS degradation, respectively. Some MAGs of *E. clostridioformis* and *E. aldenensis* encoded both SQDG/SQ and DHPS degradation pathways. Overview of known DHPS degradation pathways (c). MAG, metagenome-assembled genome; sulfo-EMP, sulfoglycolytic Embden-Meyerhof-Parnas pathway; sulfo-ED, sulfoglycolytic Entner–Doudoroff pathway; sulfo-SFT, sulfoglycolytic sulfofructose-transaldolase pathway; SQ, sulfoquinovose; DHPS, 2,3-dihydroxypropane-1-sulfonate; HpsP, DHPS-2-dehydrogenase; HpsO, DHPS-2-dehydrogenase; HpsG, DHPS-sulfolyase; HpsH, DHPS-sulfolyase activating enzyme; HpfG, DHPS-dehydratase; HpfH, DHPS-dehydratase activating enzyme; HpfD, sulfopropionaldehyde reductase; HpsN, DHPS-1-dehydrogenase; DhpA, dehydrogenase; SlaB, dehydrogenase; SuyAB sulfolactate-sulfolyase; ComC, sulfolactate dehydrogenase; SlcD, sulfolactate dehydrogenase; ComDE, 3-sulfopyruvate decarboxylase; Xsc, sulfoacetaldehyde acetyltransferase.

Enterocloster clostridioformis degrades SQ to DHPS in pure culture

Our mouse gut content microcosm experiments and genome analyses revealed members of the genus *Enterocloster* as SQ degraders. We thus performed anaerobic growth tests with the mouse strain *E. clostridioformis* YL32, which shares 100%, 99.6%, and 99.2% 16S rRNA gene sequence identity with the enriched ASVs 25, 24, and 26 in the mouse gut microcosms, respectively. Initial growth of strain YL32 in diluted or undiluted rich medium did not differ, regardless of SQ supplementation. However, cultures supplemented with SQ exhibited a

596 secondary growth phase during the late stationary phase, achieving significantly higher
597 optical densities than cultures without SQ. This secondary growth was more pronounced in
598 diluted rich medium (Figure 6 a). Diauxic growth in SQ-supplemented cultures indicated that
599 SQ supported growth only after energetically more favorable substrates in the rich medium
600 were consumed. This was supported by the timing of SQ degradation, which concurred with
601 the second growth phase after 100 h. SQ was degraded nearly stoichiometrically to DHPS
602 (Figure 6 b) while sulfide production did not differ significantly between cultures with and
603 without SQ (Figure 6 c). Although *E. clostridioformis* YL32 possesses the genetic potential to
604 ferment DHPS further (Figure 6 d), the DHPS fermentation product, 3-HPS, was not detected.

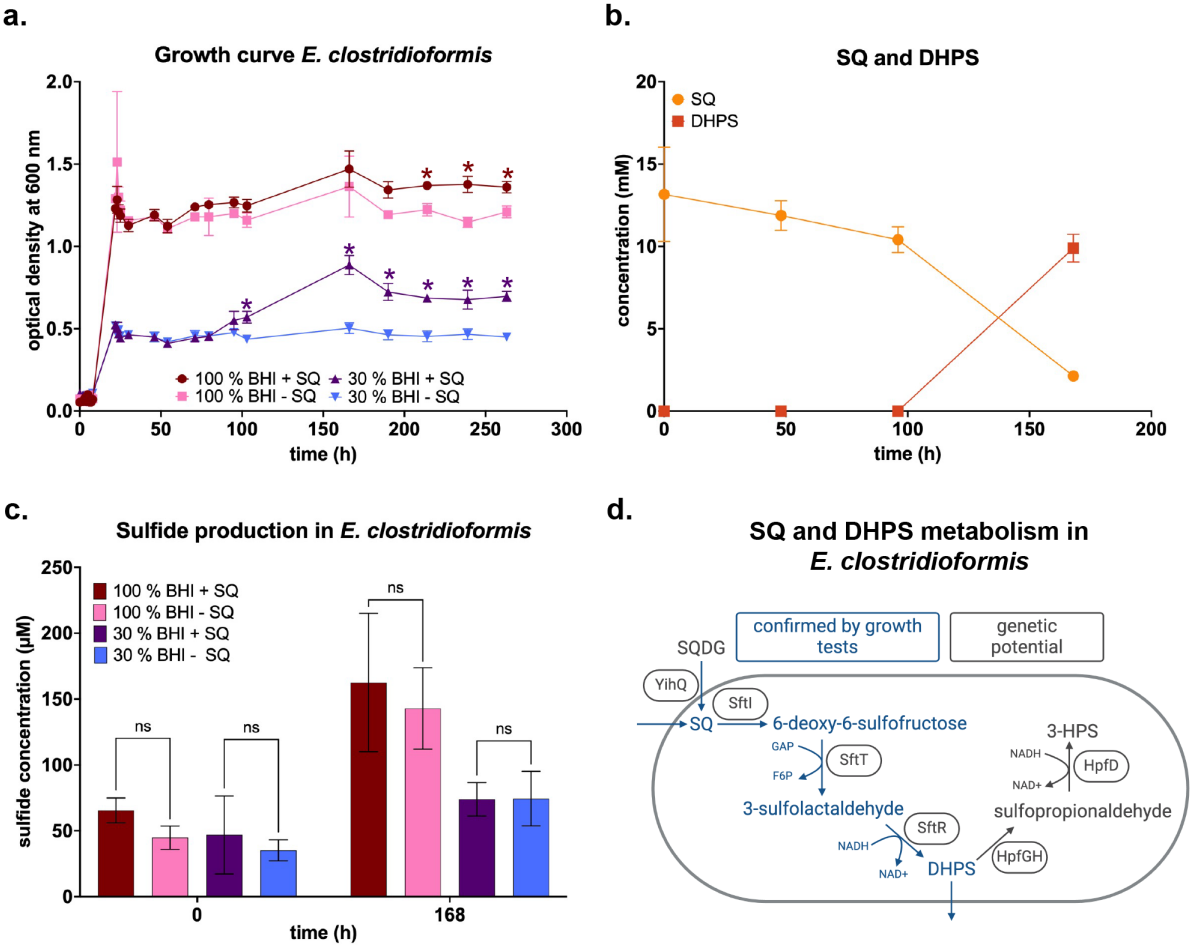

605

606 **Figure 6: A pure culture of Enterocloster clostridioformis anaerobically degraded SQ to DHPS.** Anaerobic growth tests of
607 *E. clostridioformis* strain YL32 with 10 mM SQ (a). SQ triggered a second growth phase of *E. clostridioformis* in diluted (30%)
608 rich medium (a) that coincided with a decrease of SQ and an increase of DHPS at a stoichiometry of about 1:1 (b). Small
609 amounts of sulfide were produced in all treatments but there were no significant differences between the sulfide produced
610 in incubations amended with SQ compared to unamended control incubations (c). Schematic overview of the proposed SQ

611 and DHPS pathways of *E. clostridioformis* YL32 (genome assembly number GCA_016696785) based on the growth tests and
612 genome analysis (created with biorender.com) (d). SQ can either be imported via the transporter SftA or cleaved from SQDG
613 by the sulfoquinovosidase YihQ (gene locus tag I5Q83_09300). SQ is converted to 6-deoxy-6-sulfofructose via the SQ
614 isomerase SftI (gene locus tag I5Q83_09270). The 6-deoxy-6-sulfofructose transaldolase SftT (gene locus tag I5Q83_09315)
615 catalyzes the transfer of a C3-moiety from 6-deoxy-6-sulfofructose to glyceraldehyde-3-phosphate (GAP), forming fructose
616 6-phosphate (F6P). The resulting 3-sulfolactaldehyde is then reduced to DHPS by the 3-sulfolactaldehyde reductase SftR
617 (gene locus tag I5Q83_09310). The DHPS dehydratase HpfG (gene locus tag I5Q83_10645) and its activating enzyme HpfH
618 (gene locus tag I5Q83_10640) catalyze the cleavage of the CO-bond of DHPS to form sulfopropionaldehyde, which is then
619 reduced by the sulfopropionaldehyde reductase HpfD (gene locus tag I5Q83_10625) to 3-HPS. In a., b., c., lines/bars show
620 averages of triplicate incubations with error bars representing one standard deviation. In a., coloured asterisks show
621 significant differences between treatment groups and their respective control groups without SQ. In c., brackets show non-
622 significant results in pairwise comparisons of treatment groups and their respective unamended control. Significance was
623 tested using ANOVA with Tukey's post hoc test. Adjusted *p*-values smaller than 0.05 were regarded as significant. SQ,
624 sulfoquinovose; BHI, brain-heart infusion medium; DHPS, 2,3-dihydroxypropane-1-sulfonate; 3-HPS, 3-hydroxypropane-1-
625 sulfonate; ns, not significant; SQDG, sulfoquinovosyldiacylglycerol.

626

627 Additionally, we tested SQ degradation by the mouse strain *F. rodentium* ALO17, which shares
628 100% identity with an ASV enriched in the mouse gut microcosms. However, growth of strain
629 ALO17 was not significantly different between cultures with and without SQ. Also, SQ
630 degradation and formation of degradation products were not detected (Figure S8). These
631 results are in line with the absence of known SQ and DHPS pathway genes in the *F. rodentium*
632 ALO17 genome.

633

634 Discussion

635 SQ in the gut exclusively derives from dietary intake, primarily of green edible plants (e.g.
636 spinach, green onions) and edible micro- and macroalgae (e.g. spirulina, nori) that contain the
637 ubiquitous thylakoid membrane lipid SQDG. In the mammalian gut, pancreatic lipases
638 hydrolyze SQDG to sulfoquinovosyl glycerol [54,55]. Subsequently, SQ is cleaved off from
639 SQDG or sulfoquinovosyl glycerol by sulfoquinovosidases [6,7], key enzymes of certain gut
640 bacteria that take up SQ for further respiration or fermentation. SQ (6-deoxy-6-sulfo-D-
641 glucose) is structurally analogous to glucose-6-phosphate and was initially proposed to be
642 degraded via a pathway similar to glycolysis [56,57]. Since the first discovery of sulfoglycolysis

643 in bacteria [10], further sulfoglycolytic pathways have been described in different bacterial
644 taxa [8,9,11–14]. While plants [56] and algae [58] can also degrade SQ via yet unknown
645 pathways, it was unclear if animals are capable of SQ degradation and if mammalian cells are
646 involved in intestinal SQ metabolism. Here, we show that SQ is neither metabolized by human
647 colorectal adenocarcinoma (HT-29) cells *in vitro* nor respired to CO_2 by germ-free mice *in vivo*.
648 This suggests that SQ cannot be metabolized by the mammalian host, and instead serves
649 exclusively as a nutrient and growth substrate for specialized bacteria in the animal gut.
650
651 *A. rectalis* was previously shown to be the most dominant SQ-degrading species in human
652 fecal samples. Other species, including *F. prausnitzii*, *E. aldenensis* (formerly *Clostridium*
653 *aldenense*), *E. clostridioformis* (formerly *Clostridium clostridioforme*), and *Roseburia* sp.
654 AM16-25 also contributed to transcription of sulfofructose-transaldolase pathway genes in
655 the fecal microbiome [15]. Transcription of the sulfo-Embden-Meyerhof-Parnas pathway of
656 *Enterobacteriaceae* such as *E. coli* was considerably less important. Additionally, *B.*
657 *wadsworthia* was identified as the dominant degrader of DHPS, which is produced by the
658 primary SQ fermenters [15]. Our human fecal microcosm experiments with different SQ doses
659 corroborated the relevance of *A. rectalis* and *B. wadsworthia* for complete SQ degradation to
660 H_2S in the human gut. We further revealed that a minimum concentration of 0.1 mM SQ was
661 sufficient to induce significant changes in the absolute abundance of selected microbiota
662 members. The total amount of SQ in 10 ml microcosms amended with 0.1 mM SQ
663 corresponds to the SQ content in about 11 g of fresh spinach (Table S5), the edible plant with
664 the highest known SQDG concentration [3,59]. These results align with previous findings
665 showing that SQ degradation ranks among the top third of all transcribed metabolic pathways
666 of the fecal microbiome, establishing it as a microbial core function in the human gut [15].

667 Intestinal SQ levels reached by regular dietary intake of green vegetables may thus impact gut
668 microbiota composition and potentially affect human health via SQ degradation metabolites
669 [15]. The main SQ fermentation products are formate, acetate, and DHPS [10,13,16,60].
670 Besides acetate formation, our human fecal microcosm experiments also revealed a
671 significantly higher butyrate concentration in microcosms amended with 10 mM SQ
672 compared to the control (Figure 2 f). Increased butyrate production during SQ degradation
673 has not been observed in previous SQ-amended human fecal microcosms [15], which suggests
674 it may be specific to the mixture of human fecal samples used in our study. While the reason
675 for the increased butyrate production remains unknown, it is likely produced by *A. rectalis*
676 and other bacteria that were enriched in the SQ-amended microcosms. *A. rectalis* and
677 relatives of other enriched ASVs (e.g. *W. intestinalis*) can produce butyrate from fermentation
678 of carbohydrates [61–63]. Butyrate production by *A. rectalis* involves the acetyl-CoA pathway,
679 with butyryl-CoA:acetate CoA-transferase (But) as the key terminal enzyme that generates
680 butyrate from two acetyl-CoA molecules and acetate as co-substrate [64–67]. *Faecalicatena*
681 sp. DSM22707, an isolate from petroleum reservoir produced water, produces butyrate and
682 other metabolites from SQ, highlighting butyrate as a new SQ fermentation product [38].
683 Production of SCFAs, particularly of butyrate, is considered a beneficial function of the gut
684 microbiota and a prominent effect of dietary supplementation with known prebiotics such as
685 resistant starch, inulin-type fructans, and fructooligosaccharides [68–72]. Butyrate is the
686 preferred energy source of the colonocytes [73] and has been linked to the prevention and
687 treatment of colitis [74,75] and colorectal cancer [76].
688
689 The identity and metabolic features of microorganisms involved in SQ degradation in the gut
690 of non-human animals is unknown. Laboratory mice are important models of biomedicine

691 and nutrition research. Here we demonstrate that, similar to the human gut, the capacity for
692 SQ degradation is restricted to few members of the murine microbiota. SQ is mainly degraded
693 via the sulfo-Embden-Meyerhof-Parnas pathway and the sulfofructose-transaldolase
694 pathway to DHPS. Members of the genera *Escherichia* and *Enterocloster* are primary SQ
695 degraders in the mouse gut. The more than 24 h lag phase till onset of SQ degradation in
696 mouse gut content microcosms and the absence of a significant shift in fecal microbiota
697 composition upon single-dose gavage of SQ to mice suggested that microbial SQ metabolism
698 was not active before SQ supplementation. The SQDG contents of mouse chows are not
699 known. However, the absence of SQ in feces before gavaging (Figures 1 h and 4 b) may
700 indicate that the standard mouse chow used in this study, and possibly also in other mouse
701 facilities, is not composed of foods with high SQDG content [3,77,78]. The single 1 mg and 10
702 mg SQ doses gavaged to mice correspond to the SQ content in approximately 0.37 g and 3.7
703 g of fresh spinach, which would represent about 7.5% and 75% of the total daily food intake
704 in grams of a mouse, respectively (Table S5). Mice showed no adverse effects after ingesting
705 a high SQ dose. Our results support previous findings from oral SQ supplementation
706 experiments in susceptible IL-10-deficient mice [79]. Daily gavage with 0.45 mg SQ per g body
707 weight, which corresponds roughly to the 10 mg SQ dose used in our study, over three weeks
708 did not induce changes in microbial beta-diversity and intestinal inflammation in the IL-10-
709 deficient mice [79].
710
711 Although some mouse microbiota members encode the capacity to either respire DHPS to
712 H_2S (*T. muris*, *Desulfovibrio* species) or ferment DHPS to 3-HPS (*E. clostridioformis*),
713 experiments with gut content microcosms, with conventional laboratory mice, and mouse
714 gut-derived bacterial strains did not provide evidence for active degradation of DHPS. *T. muris*

715 did not utilize DHPS in pure culture [19]. Further, *B. wadsworthia*, a confirmed DHPS degrader
716 in the human gut [15], is not widely distributed among mice and, if present, mostly derived
717 from inoculation of a human strain or human feces transplants [19]. Among the DHPS
718 degradation pathway-encoding taxa in the mouse microbiota, only *E. clostridioformis* was
719 significantly enriched in the mouse gut content microcosms. While we showed that the
720 murine *E. clostridioformis* strain YL32 ferments SQ to DHPS for growth, further degradation
721 of DHPS to 3-HPS was not observed. So-called 'extended sulfoglycolytic pathways' include
722 genes for degradation of SQ and SQ degradation products such as DHPS or sulfolactate [80].
723 For example, *E. gilvus* contains the sulfofructose-transaldolase pathway and the bifurcated
724 HpfGHD-HpfXYZ pathway for SQ and DHPS degradation [18]. *F. prausnitzii* is thought to also
725 possess an extended sulfoglycolytic pathway, as its genome encodes the sulfofructose-
726 transaldolase pathway along with a putative *hpfG* [17]. The HpfGHD pathway and the HpfXYZ
727 pathway both do not produce H_2S from DHPS [17,18]. The HpfGHD pathway does not
728 conserve energy, but regenerates NAD^+ [17], while ATP is generated in the bifurcated HpfXYZ
729 pathway [18]. Our results indicate that DHPS is not a relevant growth substrate for the gut
730 microbiota of conventional laboratory mice. Unlike the human gut, where SQ degradation
731 proceeds beyond DHPS, SQ degradation stopped at the level of DHPS in the mouse gut and
732 did not contribute to sulfide production. However, a previous study reported significant
733 sulfide production after 168 h incubation of anoxic microcosms with feces of IL-10-deficient
734 mice and 4 mM SQ, which indicated complete SQ degradation by the microbiota of this mouse
735 model [79]. Microbiota composition was not analyzed in the fecal microcosms of IL-10-
736 deficient mice. Yet, the discrepancy between the findings of this previous study and our study
737 may be attributed to differences in microbial community structure and in incubation times.
738

739 # Conclusions

740 Our work demonstrates that dietary SQ is exclusively degraded by the gut microbiota and not
741 directly metabolized by the human and murine host. We observed the enrichment of
742 commensal bacteria and significantly increased acetate and butyrate production in human
743 fecal microcosms at high physiological SQ concentrations. These results align with key criteria
744 for prebiotics [68]. SQ degradation by the gut microbiota of conventional wild type laboratory
745 mice differed fundamentally from humans, primarily by the lack of DHPS degradation.
746 Gnotobiotic animals colonized with defined consortia of microbial strains, including primary
747 and secondary SQ degraders, may be better models to study effects of complete SQ
748 degradation on the host [79]. Our study provides fundamental insight into SQ degradation in
749 the mammalian gut, and has implications for potential application of SQDG-containing foods
750 or SQ in dietary and prebiotic interventions.
751

752 # Declarations

753 ## Ethics approval and consent to participate

754 Sampling and microbial analyses of feces from healthy human adults was approved by the
755 ethics committee of the University of Vienna, Austria (reference numbers 00161 and 00714).
756 Experiments with wild type mice were approved by the national authorities in Austria
757 (Bundesministerium für Bildung, Wissenschaft und Forschung, 2022-0.745.974). Experiments
758 with germ-free mice were approved by the local authorities in Germany (Regierung von
759 Oberbayern, ROB-55.2-2532.Vet_02-19-53).

Consent for publication

Not applicable.

Availability of data and material

All sequence data generated in this project is available at NCBI under BioProject ID PRJNA1198716. The hidden Markov models developed in this project (Table S1) are available as Additional File 1.

Competing interests

The authors declare that they have no competing interests.

Funding

This research was funded by the Austrian Science Fund (FWF) [grant DOI 10.55776/DOC69 and 10.55776/COE7]. For open access purposes, the authors have applied for a CC BY public copyright license to any author-accepted manuscript version arising from this submission. BS received funding from the DFG (project no. 395357507 “SFB1371”), the European Research Council (EvoGutHealth, 865615), and the Germany Centre for Infection Research (project no. 503-5-7-06.712_00 and 503-5-7-06.709_00).

Authors' contributions

J.K. and A.L. conceived the study. J.K., B.T.H., A.S.W., S.B., M.L., and G.A. performed experiments and analyzed data. A.R., D.B., D.M., D.S., and B.S. contributed essential experimental infrastructure and analytical instrumentation, and expert advice. J.K., T.S.T., and

779 B.H. performed bioinformatic analyses. J.K., B.T.H., A.S.W., S.B., T.S.T., M.M., and A.L.
780 interpreted the data. J.K., M.M., and A.L. wrote the article. All authors revised and approved
781 the manuscript.

782 **Acknowledgements**

783 We thank the staff of the Joint Microbiome Facility for sequencing and Margarete Watzka for
784 isotope ratio mass spectrometry measurements.

785

786 # References

787 1. Harwood JL, Nicholls RG. The plant sulpholipid—a major component of the sulphur cycle.
788 Biochem Soc Trans. 1979;7:440–7.

789 2. Snow AJD, Burchill L, Sharma M, Davies GJ, Williams SJ. Sulfoglycolysis: catabolic pathways
790 for metabolism of sulfoquinovose. Chem Soc Rev. 2021;50:13628–45.

791 3. Goddard-Borger ED, Williams SJ. Sulfoquinovose in the biosphere: occurrence, metabolism
792 and functions. Biochem J. 2017;474:827–49.

793 4. Sato N, Aoki M, Maru Y, Sonoike K, Minoda A, Tsuzuki M. Involvement of sulfoquinovosyl
794 diacylglycerol in the structural integrity and heat-tolerance of photosystem II. Planta.
795 2003;217:245–51.

796 5. Nakajima Y, Umena Y, Nagao R, Endo K, Kobayashi K, Akita F, *et al*. Thylakoid membrane
797 lipid sulfoquinovosyl-diacylglycerol (SQDG) is required for full functioning of photosystem II
798 in *Thermosynechococcus elongatus*. J Biol Chem. 2018;293:14786–97.

799 6. Speciale G, Jin Y, Davies GJ, Williams SJ, Goddard-Borger ED. YihQ is a sulfoquinovosidase
800 that cleaves sulfoquinovosyl diacylglyceride sulfolipids. Nat Chem Biol. 2016;12:215–7.

801 7. Kaur A, Pickles IB, Sharma M, Madeido Soler N, Scott NE, Pidot SJ, *et al*. Widespread Family
802 of NAD+-Dependent Sulfoquinovosidases at the Gateway to Sulfoquinovose Catabolism. J Am
803 Chem Soc. 2023;145:28216–23.

804 8. Sharma M, Lingford JP, Petricevic M, Snow AJD, Zhang Y, Järvå MA, *et al*. Oxidative
805 desulfurization pathway for complete catabolism of sulfoquinovose by bacteria. Proc Natl
806 Acad Sci USA. 2022;119.

807 9. Ye Z, Wei Y, Jiang L, Zhang Y. Oxygenolytic sulfoquinovose degradation by an iron-
808 dependent alkanesulfonate dioxygenase. iScience. 2023;26:107803.

809 10. Denger K, Weiss M, Felux A-K, Schneider A, Mayer C, Spiteller D, *et al*. Sulphoglycolysis in
810 *Escherichia coli* K-12 closes a gap in the biogeochemical sulphur cycle. Nature. 2014;507:114–
811 7.

812 11. Liu J, Wei Y, Ma K, An J, Liu X, Liu Y, *et al*. Mechanistically diverse pathways for
813 sulfoquinovose degradation in bacteria. ACS Catal. 2021;11:14740–50.

814 12. Felux A-K, Spiteller D, Klebensberger J, Schleheck D. Entner-Doudoroff pathway for
815 sulfoquinovose degradation in *Pseudomonas putida* SQ1. Proc Natl Acad Sci USA.
816 2015;112:E4298-305.

817 13. Frommeyer B, Fiedler AW, Oehler SR, Hanson BT, Loy A, Franchini P, *et al*. Environmental
818 and intestinal phylum Firmicutes bacteria metabolize the plant sugar sulfoquinovose via a 6-
819 deoxy-6-sulfofructose transaldolase pathway. iScience. 2020;23:101510.

820 14. Liu Y, Wei Y, Zhou Y, Ang EL, Zhao H, Zhang Y. A transaldolase-dependent sulfoglycolysis
821 pathway in *Bacillus megaterium* DSM 1804. Biochem Biophys Res Commun. 2020;533:1109–
822 14.

823 15. Hanson BT, Dimitri Kits K, Löffler J, Burrichter AG, Fiedler A, Denger K, *et al*. Sulfoquinovose
824 is a select nutrient of prominent bacteria and a source of hydrogen sulfide in the human gut.
825 ISME J. 2021;15:2779–91.

826 16. Burrichter A, Denger K, Franchini P, Huhn T, Müller N, Spiteller D, *et al*. Anaerobic
827 degradation of the plant sugar sulfoquinovose concomitant with H_2S production: *Escherichia*
828 *coli* K-12 and *Desulfovibrio* sp. strain DF1 as co-culture model. Front Microbiol. 2018;9:2792.

829 17. Liu J, Wei Y, Lin L, Teng L, Yin J, Lu Q, *et al*. Two radical-dependent mechanisms for
830 anaerobic degradation of the globally abundant organosulfur compound
831 dihydroxypropanesulfonate. Proc Natl Acad Sci USA. 2020;117:15599–608.

832 18. Chen Y, Chu R, Ma K, Jiang L, Yang Q, Li Z, *et al*. Study of sulfoglycolysis in *Enterococcus*
833 *gilvus* reveals a widespread bifurcated pathway for dihydroxypropanesulfonate degradation.
834 iScience. 2024;111010.

835 19. Ye H, Borusak S, Eberl C, Krasenbrink J, Weiss AS, Chen S-C, *et al*. Ecophysiology and
836 interactions of a taurine-respiring bacterium in the mouse gut. Nat Commun. 2023;14:5533.

837 20. Mayer J, Huhn T, Habeck M, Denger K, Hollemeyer K, Cook AM. 2,3-Dihydroxypropane-1-
838 sulfonate degraded by *Cupriavidus pinatubonensis* JMP134: purification of
839 dihydroxypropanesulfonate 3-dehydrogenase. Microbiology. 2010;156:1556–64.

840 21. Denger K, Cook AM. Racemase activity effected by two dehydrogenases in sulfolactate
841 degradation by *Chromohalobacter salexigens*: purification of (S)-sulfolactate dehydrogenase.
842 Microbiology. 2010;156:967–74.

843 22. Pasolli E, Asnicar F, Manara S, Zolfo M, Karcher N, Armanini F, *et al*. Extensive unexplored
844 human microbiome diversity revealed by over 150,000 genomes from metagenomes
845 spanning age, geography, and lifestyle. Cell. 2019;176:649-662.e20.

846 23. Dikeocha IJ, Al-Kabsi AM, Chiu H-T, Alshawsh MA. *Faecalibacterium prausnitzii*
847 ameliorates colorectal tumorigenesis and suppresses proliferation of HCT116 colorectal
848 cancer cells. Biomedicines. 2022;10:1128.

849 24. Zeevi D, Korem T, Zmora N, Israeli D, Rothschild D, Weinberger A, *et al*. Personalized
850 nutrition by prediction of glycemic responses. Cell. 2015;163:1079–94.

851 25. Banerjee R. Hydrogen sulfide: redox metabolism and signaling. Antioxid Redox Signal.
852 2011;15:339–41.

853 26. Blachier F, Beaumont M, Kim E. Cysteine-derived hydrogen sulfide and gut health: a
854 matter of endogenous or bacterial origin. Curr Opin Clin Nutr Metab Care. 2019;22:68–75.

855 27. Olson KR, Straub KD. The role of hydrogen sulfide in evolution and the evolution of
856 hydrogen sulfide in metabolism and signaling. Physiology. 2016;31:60–72.

857 28. Stacy A, Andrade-Oliveira V, McCulloch JA, Hild B, Oh JH, Perez-Chaparro PJ, *et al*. Infection
858 trains the host for microbiota-enhanced resistance to pathogens. Cell. 2021;184:615-627.e17.

859 29. Ijssennagger N, Belzer C, Hooiveld GJ, Dekker J, van Mil SWC, Müller M, *et al.* Gut
860 microbiota facilitates dietary heme-induced epithelial hyperproliferation by opening the
861 mucus barrier in colon. Proc Natl Acad Sci USA. 2015;112:10038–43.

862 30. Beauchamp RO Jr, Bus JS, Popp JA, Boreiko CJ, Andjelkovich DA. A critical review of the
863 literature on hydrogen sulfide toxicity. Crit Rev Toxicol. 1984;13:25–97.

864 31. Devkota S, Wang Y, Musch MW, Leone V, Fehlner-Peach H, Nadimpalli A, *et al*. Dietary-
865 fat-induced taurocholic acid promotes pathobiont expansion and colitis in Il10-/- mice.
866 Nature. 2012;487:104–8.

867 32. Carbonero F, Benefiel AC, Alizadeh-Ghamsari AH, Gaskins HR. Microbial pathways in
868 colonic sulfur metabolism and links with health and disease. Front Physiol. 2012;3:448.

869 33. Vichai V, Kirtikara K. Sulforhodamine B colorimetric assay for cytotoxicity screening. Nat
870 Protoc. 2006;1:1112–6.

871 34. Brugiroux S, Beutler M, Pfann C, Garzetti D, Ruscheweyh H-J, Ring D, *et al*. Genome-guided
872 design of a defined mouse microbiota that confers colonization resistance against *Salmonella*
873 *enterica* serovar Typhimurium. Nat Microbiol. 2016;2:16215.

874 35. Gronbach K, Flade I, Holst O, Lindner B, Ruscheweyh HJ, Wittmann A, *et al*. Endotoxicity
875 of lipopolysaccharide as a determinant of T-cell-mediated colitis induction in mice.
876 Gastroenterology. 2014;146:765–75.

877 36. Zhang Y, Mui JW-Y, Arumaperuma T, Lingford JP, Goddard-Borger ED, White JM, *et al*.
878 Concise synthesis of sulfoquinovose and sulfoquinovosyl diacylglycerides, and development

879 of a fluorogenic substrate for sulfoquinovosidases. Org Biomol Chem. 2020;18:675–86.

880 37. Cline JD. Spectrophotometric determination of hydrogen sulfide in natural waters. Limnol
881 Oceanogr. 1969;14:454–8.

882 38. Borusak S, Denger K, Dorendorf T, Fournier C, Lerner H, Mayans O, *et al*. Anaerobic
883 *Faecalicatena* spp. degrade sulfoquinovose via a bifurcated 6-deoxy-6-sulfofructose
884 transketolase/transaldolase pathway to both C_2- and C_3-sulfonate intermediates. Front
885 Microbiol. 2024;15:1491101.

886 39. Pjevac P, Hausmann B, Schwarz J, Kohl G, Herbold CW, Loy A, *et al*. An economical and
887 flexible dual barcoding, two-step PCR approach for highly multiplexed amplicon sequencing.
888 Front Microbiol. 2021;12:669776.

889 40. Herbold CW, Pelikan C, Kuzyk O, Hausmann B, Angel R, Berry D, *et al*. A flexible and
890 economical barcoding approach for highly multiplexed amplicon sequencing of diverse target
891 genes. Front Microbiol. 2015;6:731.

892 41. Callahan BJ, McMurdie PJ, Rosen MJ, Han AW, Johnson AJA, Holmes SP. DADA2: High-
893 resolution sample inference from Illumina amplicon data. Nat Methods. 2016;13:581–3.

894 42. McMurdie PJ, Holmes S. phyloseq: an R package for reproducible interactive analysis and
895 graphics of microbiome census data. PLoS One. 2013;8:e61217.

896 43. Oksanen J. vegan : community ecology package-R package version 1.17-8. http://CRANR-
897 project.org/package=vegan. 2011. Accessed 12 Jun 2024.

898 44. Love MI, Huber W, Anders S. Moderated estimation of fold change and dispersion for RNA-
899 seq data with DESeq2. Genome Biol. 2014;15:550.

900 45. Sayers EW, Bolton EE, Brister JR, Canese K, Chan J, Comeau DC, *et al*. Database resources
901 of the national center for biotechnology information. Nucleic Acids Res. 2022;50:D20–6.

902 46. Parada AE, Needham DM, Fuhrman JA. Every base matters: assessing small subunit rRNA
903 primers for marine microbiomes with mock communities, time series and global field
904 samples. Environ Microbiol. 2016;18:1403–14.

905 47. Apprill A, McNally S, Parsons R, Weber L. Minor revision to V4 region SSU rRNA 806R gene
906 primer greatly increases detection of SAR11 bacterioplankton. Aquat Microb Ecol.
907 2015;75:129–37.

908 48. Beresford-Jones BS, Forster SC, Stares MD, Notley G, Viciani E, Browne HP, *et al*. The
909 Mouse Gastrointestinal Bacteria Catalogue enables translation between the mouse and
910 human gut microbiotas via functional mapping. Cell Host Microbe. 2022;30:124-138.e8.

911 49. Tanabe TS, Dahl C. HMSS2: An advanced tool for the analysis of sulphur metabolism,
912 including organosulphur compound transformation, in genome and metagenome assemblies.
913 Mol Ecol Resour. 2023;23:1930–45.

914 50. Tanabe TS, Dahl C. HMS-S-S: A tool for the identification of sulphur metabolism-related

915 genes and analysis of operon structures in genome and metagenome assemblies. Mol Ecol
916 Resour. 2022;22:2758–74.

917 51. Morimoto Y, Uesaka K, Fujita Y, Yamamoto H. A nitrogenase-like enzyme is involved in the
918 novel anaerobic assimilation pathway of a sulfonate, isethionate, in the photosynthetic
919 bacterium *Rhodobacter capsulatus*. mSphere. 2024;9:e00498-24.

920 52. An J, Wei Y, Liu J, Lui Ang E, Zhao H, Zhang Y. Biochemical investigation of 3-
921 sulfopropionaldehyde reductase HpfD. Chembiochem. 2021;22:2862–6.

922 53. Svetlitsky D, Dagan T, Ziv-Ukelson M. Discovery of multi-operon colinear syntenic blocks
923 in microbial genomes. Bioinformatics. 2020;36:i21–9.

924 54. Gupta SD, Sastry PS. Metabolism of the plant sulfolipid--sulfoquinovosyldiacylglycerol:
925 degradation in animal tissues. Arch Biochem Biophys. 1987;259:510–9.

926 55. Andersson L, Bratt C, Arnoldsson KC, Herslöf B, Olsson NU, Sternby B, *et al*. Hydrolysis of
927 galactolipids by human pancreatic lipolytic enzymes and duodenal contents. J Lipid Res.
928 1995;36:1392–400.

929 56. Benson AA, Lee RF. The sulphoglycolytic pathway in plants. Biochem J. 1972;128:29P-30P.

930 57. Roy AB, Hewlins MJE, Ellis AJ, Harwood JL, White GF. Glycolytic breakdown of
931 sulfoquinovose in bacteria: a missing link in the sulfur cycle. Appl Environ Microbiol.
932 2003;69:6434–41.

933 58. Scholz S, Serif M, Schleheck D, Sayer MDJ, Cook AM, Küpper FC. Sulfoquinovose
934 metabolism in marine algae. Botanica Marina. 2021;64:301–12.

935 59. Kuriyama I, Musumi K, Yonezawa Y, Takemura M, Maeda N, Iijima H, *et al*. Inhibitory
936 effects of glycolipids fraction from spinach on mammalian DNA polymerase activity and
937 human cancer cell proliferation. J Nutr Biochem. 2005;16:594–601.

938 60. Sharma M, Abayakoon P, Epa R, Jin Y, Lingford JP, Shimada T, *et al*. Molecular basis of
939 sulfosugar selectivity in sulfoglycolysis. ACS Cent Sci. 2021;7:476–87.

940 61. Fu X, Liu Z, Zhu C, Mou H, Kong Q. Nondigestible carbohydrates, butyrate, and butyrate-
941 producing bacteria. Crit Rev Food Sci Nutr. 2019;59:S130–52.

942 62. Sakamoto M, Hisatomi A, Ohkuma M. Isolation and characterization of a novel *Waltera*
943 species and reclassification of *Brotolimicola acetigignens* Hitch *et al*. 2022 as *Waltera*
944 *acetigignens* comb. nov. Int J Syst Evol Microbiol. 2024;74:006381.

945 63. Van-Wehle T, Vital M. Investigating the response of the butyrate production potential to
946 major fibers in dietary intervention studies. NPJ Biofilms Microbiomes. 2024;10:63.

947 64. Barcenilla A, Pryde SE, Martin JC, Duncan SH, Stewart CS, Henderson C, *et al*. Phylogenetic
948 relationships of butyrate-producing bacteria from the human gut. Appl Environ Microbiol.
949 2000;66:1654–61.

950 65. Duncan SH, Barcenilla A, Stewart CS, Pryde SE, Flint HJ. Acetate utilization and butyryl
951 coenzyme A (CoA):acetate-CoA transferase in butyrate-producing bacteria from the human
952 large intestine. Appl Environ Microbiol. 2002;68:5186–90.

953 66. Louis P, Young P, Holtrop G, Flint HJ. Diversity of human colonic butyrate-producing
954 bacteria revealed by analysis of the butyryl-CoA:acetate CoA-transferase gene. Environ
955 Microbiol. 2010;12:304–14.

956 67. Louis P, Duncan SH, McCrae SI, Millar J, Jackson MS, Flint HJ. Restricted distribution of the
957 butyrate kinase pathway among butyrate-producing bacteria from the human colon. Journal
958 of Bacteriology. 2004; 186(7):2099-106.

959 68. Hutkins R, Walter J, Gibson GR, Bedu-Ferrari C, Scott K, Tancredi DJ, *et al*. Classifying
960 compounds as prebiotics - scientific perspectives and recommendations. Nat Rev
961 Gastroenterol Hepatol. 2024;1–17.

962 69. DeMartino P, Cockburn DW. Resistant starch: impact on the gut microbiome and health.
963 Curr Opin Biotechnol. 2020;61:66–71.

964 70. Timm DA, Stewart ML, Hospattankar A, Slavin JL. Wheat dextrin, psyllium, and inulin
965 produce distinct fermentation patterns, gas volumes, and short-chain fatty acid profiles in
966 vitro. J Med Food. 2010;13:961–6.

967 71. Roberfroid MB. Introducing inulin-type fructans. Br J Nutr. 2005;93 Suppl 1:S13-25.

968 72. Hosoya N, Dhorranintra B, Hidaka H. Utilization of [U-^{14}C]fructooligosaccharides in man as
969 energy resources. Journal of Clinical Biochemistry and Nutrition. 1988;5:67–74.

970 73. Hodgkinson K, El Abbar F, Dobranowski P, Manoogian J, Butcher J, Figeys D, *et al*.
971 Butyrate's role in human health and the current progress towards its clinical application to
972 treat gastrointestinal disease. Clin Nutr. 2023;42:61–75.

973 74. Recharla N, Geesala R, Shi X-Z. Gut microbial metabolite butyrate and its therapeutic role
974 in inflammatory bowel disease: A literature review. Nutrients. 2023;15(10):2275.

975 75. Segain JP, Raingeard de la Blétière D, Bourreille A, Leray V, Gervois N, Rosales C, *et al*.
976 Butyrate inhibits inflammatory responses through NFkappaB inhibition: implications for
977 Crohn's disease. Gut. 2000;47:397–403.

978 76. Kang J, Sun M, Chang Y, Chen H, Zhang J, Liang X, *et al*. Butyrate ameliorates colorectal
979 cancer through regulating intestinal microecological disorders. Anticancer Drugs.
980 2023;34:227–37.

981 77. Weidmann E, Samadi N, Klems M, Heiden D, Seppova K, Ret D, *et al*. Mouse chow
982 composition influences immune responses and food allergy development in a mouse model.
983 Nutrients. 2018;10:1775.

984 78. Whelan J, Whelan J. Conversion of dietary polyunsaturated fats between humans and
985 rodents: A review of allometric scaling models. Prostaglandins Leukot Essent Fatty Acids.

986 2020;158:102094.

987 79. Burkhardt W, Rausch T, Klopfleisch R, Blaut M, Braune A. Impact of dietary sulfolipid-
988 derived sulfoquinovose on gut microbiota composition and inflammatory status of colitis-
989 prone interleukin-10-deficient mice. Int J Med Microbiol. 2021;311:151494.

990 80. Wei Y, Tong Y, Zhang Y. New mechanisms for bacterial degradation of sulfoquinovose.
991 Biosci Rep. 2022;42(10):BSR20220314.